

Parameterization of Pressure Perturbations in a PBL Mass-Flux Model

CARA-LYN LAPPEN AND DAVID A. RANDALL

Department of Atmospheric Sciences, Colorado State University, Fort Collins, Colorado

(Manuscript received 21 July 2005, in final form 9 November 2005)

ABSTRACT

In a companion paper, the authors presented a boundary layer parameterization that was based on the mass-flux concept and included an internally consistent representation of the vertical flux of horizontal momentum. In the present paper, the authors show how the framework of that model can be used to determine the perturbation pressure field, by solving the anelastic pressure equation. The pressure covariances needed to close the parameterization can then be diagnosed. Tests show very encouraging agreement of the pressure statistics with results obtained from large-eddy simulations.

1. Introduction

In 2001, we (Lappen and Randall 2001a–c, hereafter LR01a,b,c, respectively) described a new type of mass-flux model called assumed distributions with higher-order closure (ADHOC). ADHOC is a planetary boundary layer mass-flux model. The first version of ADHOC, hereafter ADHOC1, predicted the vertical fluxes of energy and moisture, but the vertical flux of horizontal momentum was determined using conventional second-order closure methods. Similarly, although ADHOC's equations contain terms involving covariances between pressure and other variables (hereafter, the pressure terms), ADHOC1 did not incorporate these terms into the mass-flux framework. Instead, the pressure terms were determined using Launder's parameterization modified by Zeman and Lumley (Launder 1975; Launder et al. 1975, hereafter L75; Zeman and Lumley 1979, hereafter ZL79). In a companion paper (Lappen and Randall 2005, hereafter LR05), we describe ADHOC2, which includes consistent representations of the momentum fluxes. The current paper builds on the results of LR05 to derive parameterizations of the pressure terms.

Following LR05, we consider idealized versions of two coherent structures that are commonly observed in the PBL, namely plumes (cylindrical geometry with major axis perpendicular to the ground) and rolls

(quasi-cylindrical geometry with major axis parallel to the ground). We use the assumed geometries of these coherent structures to derive velocity fields, and solve the anelastic pressure equation to obtain the pressure fields. The covariances needed in the model are then constructed directly, by integration. Our methods require as input certain information (discussed later) about the updrafts and downdrafts; this information is available in ADHOC2. It can also be diagnosed from large-eddy simulation (LES) results, which we use to test our parameterization. In addition, we compare our results to those obtained with previously published parameterizations of the pressure terms. Note, however, that our parameterization can be used only with mass-flux models of the PBL.

In the derivation of the parameterizations we present, we have chosen for simplicity to neglect the following two potential sources of pressure perturbations: 1) vorticity-induced pressure perturbations, and 2) pressure perturbations arising from internal gravity waves generated by thermal convection. While we acknowledge that these can be important, we have tried to simplify the cases as much as possible to provide a framework for attacking this problem in mass-flux PBL models. We later hope to extend the framework to include these aforementioned effects.

An outline of this paper is as follows: In section 2, we discuss the case of axisymmetric convection with no shear. In section 3, we examine a slab-symmetric case with both buoyancy and shear. In each of these sections, we compare results from the current parameterization, the Rotta (1951, hereafter R51) and L75/ZL79

Corresponding author address: Cara-Lyn Lappen, 87 Sortais Road, Durango, CO 81301.
E-mail: lappen@atmos.colostate.edu

parameterizations, and LES. Section 4 gives a critique of our parameterization, and a discussion of its limitations.

2. Axisymmetric free convection

Axisymmetric convective plumes (Fig. 1a) occur in free convective PBLs, as is well known on the basis of both observations (e.g., Willis and Deardorff 1974) and LES (e.g., Moeng 1984). To describe a plume, we adopt cylindrical coordinates, with radial coordinate r . The inner cylinder has radius $r = R_i(z)$, while the radius of the outer cylinder, that is, the total diameter of the plume, is denoted by R_o . We assume that R_o is independent of height; this assumption can be interpreted to mean that the plumes are closely packed. Let σ_i denote the fractional area occupied by the inner cylinder (hereafter, subscripts i and o denote inner and outer, respectively), so that

$$\sigma_i(z) = \frac{R_i^2(z)}{R_o^2}. \quad (1)$$

Let v_r , v_ϕ , and w be the radial, azimuthal, and vertical components of the perturbation velocity, that is, $\mathbf{v} = v_r \hat{\mathbf{r}} + v_\phi \hat{\boldsymbol{\phi}} + w \hat{\mathbf{z}}$. We assume that there is no azimuthal motion, that is,

$$v_\phi \equiv 0. \quad (2)$$

Using this assumption implies that we are considering plumes without vorticity. We realize that this is not ideal, but the case we will test for this parameterization has nearly zero mean flow and minimal vorticity. It is thus a good approximation for this particular case. With a plume that was more vortical in nature, we would need to include the azimuthal component of the velocity. With this assumption, the Boussinesq form of the continuity equation can be written as

$$\frac{\partial}{\partial r}(rv_r) + \frac{\partial}{\partial z}(wr) = 0. \quad (3)$$

From (3), and using the assumption that w is horizontally uniform within the updraft and downdraft, LR05 show that

$$v_r(r) = -\frac{r}{2} \frac{\partial w_u}{\partial z} \quad \text{for } r < R_i; \quad (4)$$

$$(v_r)_{R_i+\varepsilon} = (v_r)_{R_i-\varepsilon} + (w_d - w_u) \frac{\partial R_i}{\partial z}; \quad (5)$$

and

$$rv_r(r) = \left(\frac{R_o^2 - r^2}{2} \right) \frac{\partial w_d}{\partial z} \quad \text{for } R_i < r \leq R_o. \quad (6)$$

In Eqs. (4)–(6), we assume that the inner (outer) cylinder is the updraft (downdraft), that is, $w_i = w_u$ and

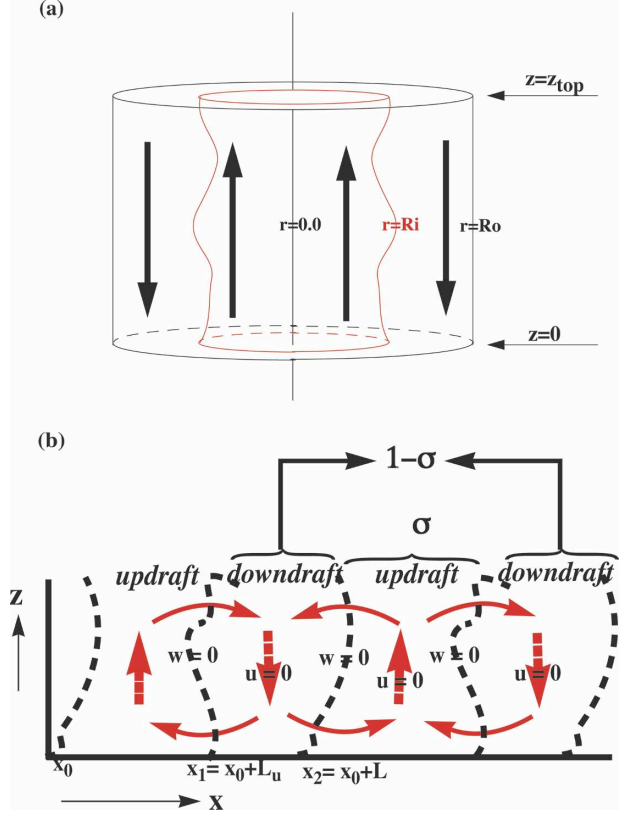


FIG. 1. Idealization of (a) the clear convective geometry and (b) the slab symmetric roll geometry. In (a), the inner and outer cylinders are concentric circles and R_i (R_o) is the distance from the updraft center to the outer edge of the updraft (downdraft). Note that R_i varies with height but R_o does not. In (b), a cross section through the major axes of the rolls is shown; L_u and L_d are the widths of the updraft and downdraft, respectively, and x_1 represents border where an updraft becomes a downdraft. Similarly, x_0 and x_2 represent borders where downdrafts become updrafts.

$w_o = w_d$. We note, however, that the parameterization still holds if we assume that the opposite is true. To determine $v_r(r, z)$, we need know $w_u(z)$, $w_d(z)$, R_o , and $R_i(z) = \sqrt{\sigma_i(z)} R_o$. LR05 show how to determine these quantities from the prognostic variables of ADHOC2. In the present paper, we treat them as known.

With the assumptions of axisymmetry and no azimuthal motion, and neglecting rotation and friction, the equation of radial motion with the Boussinesq approximation is

$$\frac{\partial v_r}{\partial t} + v_r \frac{\partial v_r}{\partial r} + w \frac{\partial v_r}{\partial z} = -\frac{\partial}{\partial r} \left(\frac{p'}{\rho} \right). \quad (7)$$

In (7), we have also neglected the subplume-scale turbulent transport term. We are not neglecting subplume-scale turbulent transport itself, but the term that will be the radial derivative of the turbulent transport in the elliptical pressure equation [Eq. (10)]. We do this

purely for simplicity as we test the feasibility of this approach. In LR01b we discuss the handling of the subplume-scale transport term in ADHOC2. In (7), p' is the perturbation pressure, which is the departure from a hydrostatically balanced basic-state pressure. Obviously, if the system is in a steady resting state, $(\partial/\partial t)[(p'/\rho)] = 0$ everywhere.

Similarly, the equation of vertical motion is

$$\frac{\partial w}{\partial t} + v_r \frac{\partial w}{\partial r} + w \frac{\partial w}{\partial z} = -\frac{\partial}{\partial z} \left(\frac{p'}{\rho} \right) + g \frac{\theta'_v}{\theta_0}, \quad (8)$$

where g is the acceleration of gravity, θ'_v is the perturbation virtual potential temperature, and θ_0 is a reference potential temperature. We assume that nonzero values of θ'_v are due only to the convective motions. With this assumption, we see that for a steady, resting state, (8) reduces to

$$0 = -\frac{\partial}{\partial z} \left(\frac{p'}{\rho} \right). \quad (9)$$

By combining (7), (8), and (3), we can derive the elliptic equation satisfied by the pressure, hereafter the pressure equation, in cylindrical coordinates:

$$\begin{aligned} \frac{1}{r} \frac{\partial}{\partial r} \left[r \frac{\partial}{\partial r} \left(\frac{p'}{\rho} \right) \right] + \frac{\partial^2}{\partial z^2} \left(\frac{p'}{\rho} \right) = \\ - \left[\left(\frac{\partial v_r}{\partial r} \right)^2 + 2 \frac{\partial w}{\partial r} \frac{\partial v_r}{\partial z} + \left(\frac{\partial w}{\partial z} \right)^2 + \left(\frac{v_r}{r} \right)^2 \right] + B. \end{aligned} \quad (10)$$

Here we define

$$B \equiv \frac{g}{\theta_0} \frac{\partial \theta'_v}{\partial z}, \quad (11)$$

and assume that the area average of B is equal to zero, that is,

$$\bar{B} = 0. \quad (12)$$

For a resting state, we get

$$\frac{1}{r} \frac{\partial}{\partial r} \left[r \frac{\partial}{\partial r} \left(\frac{p'}{\rho} \right) \right] + \frac{\partial^2}{\partial z^2} \left(\frac{p'}{\rho} \right) = 0. \quad (13)$$

We will solve Eq. (10) separately in the updraft and downdraft. Thus, we need four horizontal (radial) boundary conditions. We also need two vertical boundary conditions. The four boundary conditions can be derived as follows. Since $v_r = 0$ for all time at $r = 0$ (the center of the updraft), Eq. (7) implies that

$$\left(\frac{\partial}{\partial r} p' \right)_{r=0} = 0. \quad (14)$$

Similarly, our assumption that the plumes are close-packed implies that $v_r = 0$ at $r = R_o$, and it follows from (7) that

$$\left(\frac{\partial}{\partial r} p' \right)_{r=R_o} = 0. \quad (15)$$

For isolated plumes in a quiescent environment, (15) would be replaced by $p' = 0$ at $r = R_o$.

The pressure must be continuous at $r = R_i$; that is,

$$\lim_{\varepsilon \rightarrow 0} p'(R_i + \varepsilon) = \lim_{\varepsilon \rightarrow 0} p'(R_i - \varepsilon), \quad (16)$$

where ε is a small number. The fourth condition that we use is that the area-averaged perturbation pressure is equal to zero; that is,

$$\bar{p}' = 0. \quad (17)$$

While this may not be exactly true, it is approximately true since the perturbation pressures are much smaller than the average pressure field. We note here that the parameterization will work for any value of \bar{p}' as long as its value is known.

Finally, hydrostatic balance is required at both the top of the model and the lower boundary. It follows from (8) that

$$\left(\frac{\partial}{\partial z} p' \right)_{z=z_{\text{top}}} = \left(\rho_0 g \frac{\theta'_v}{\theta_0} \right)_{z=z_{\text{top}}}. \quad (18)$$

and

$$\left(\frac{\partial}{\partial z} p' \right)_{z=0} = \left(\rho_0 g \frac{\theta'_v}{\theta_0} \right)_{z=0}. \quad (19)$$

To solve (10) subject to the boundary conditions (14)–(19), we use an analytical method to represent (and solve for) the horizontal structure, and a finite-difference method to represent the vertical structure. We begin by radially integrating Eq. (10) separately for the inner and outer regions, using our (mass-flux) assumption that the vertical velocity and potential temperature are horizontally uniform within the updraft and the downdraft. The buoyancy forcing can be separated into horizontally uniform updraft and downdraft parts:

$$B_u = \frac{g}{\theta_0} \frac{\partial(\theta'_v)_u}{\partial z} \quad \text{and} \quad B_d = \frac{g}{\theta_0} \frac{\partial(\theta'_v)_d}{\partial z}. \quad (20)$$

As shown in appendix A, the solutions are

$$\begin{aligned} \frac{p'(r)}{\rho} = \frac{p'(0)}{\rho} + B_u \left(\frac{r^2}{4} \right) - \frac{3r^2}{8} \left(\frac{\partial w_u}{\partial z} \right)^2 \\ - \frac{\partial^2}{\partial z^2} \left\{ \int_0^r \frac{1}{r} \left[\int_0^r (rp) dr \right] dr \right\} \quad \text{for } r \leq R_i; \end{aligned} \quad (21)$$

and

$$\begin{aligned}
 \frac{p'(r)}{\rho} &= \frac{p'(0)}{\rho} + \left\{ R_i \left[\frac{\partial}{\partial r} \left(\frac{p'}{\rho} \right) \right]_{R_i+\varepsilon} \right. \\
 &+ \frac{1}{4} \left(-\frac{R_o^4}{R_i^2} + 3R_i^2 \right) \left(\frac{\partial w_d}{\partial z} \right)^2 - \frac{B_d}{2} R_i^2 \left. \right\} \ln \left(\frac{r}{R_i} \right) - \frac{1}{8} \left(\frac{\partial w_d}{\partial z} \right)^2 \left[R_o^4 \left(\frac{1}{r^2} - \frac{1}{R_i^2} \right) + 3(r^2 - R_i^2) \right] + \frac{(r^2 - R_i^2)}{4} B_d \\
 &+ B_u \left(\frac{R_i^2}{4} \right) - \frac{3R_i^2}{8} \left(\frac{\partial w_u}{\partial z} \right)^2 - \frac{\partial^2}{\partial z^2} \left\{ \int_0^{(R_i-\varepsilon)} \frac{1}{r} \left[\int_0^r (rp) dr \right] dr + \int_{(R_i+\varepsilon)}^r \frac{1}{r} \left[\int_{(R_i+\varepsilon)}^r (rp) dr \right] dr \right\} \\
 &+ \left\{ R_i p(R_i) \frac{\partial^2 R_i}{\partial z^2} + 2 \frac{\partial}{\partial z} [R_i p(R_i)] \frac{\partial R_i}{\partial z} \right\} \ln \frac{r}{R_i} - \left(\frac{\partial^2 R_i}{\partial z^2} \right) \left[\frac{1}{R_i} \int_0^{(R_i-\varepsilon)} (rp) dr \right] \\
 &- 2 \left(\frac{\partial R_i}{\partial z} \right) \frac{\partial}{\partial z} \left[\frac{1}{R_i} \int_0^{(R_i-\varepsilon)} (rp) dr \right] \quad \text{for } R_i < r \leq R_o.
 \end{aligned} \tag{22}$$

There is no contribution to p at $r = R_i$ because $(\partial p/\partial r)$ is a step function there. In Eqs. (21)–(22), $p'(0)$ is a constant of integration.

The total solution for the pressure is given by Eqs. (21) and (22). In these equations, the terms involving the integrals are solved using finite difference methods (discussed in section 2a). The first term in the curly brackets of Eq. (22) is known [see appendix A, Eq. (A23)]. The rest of the quantities with the exception of $p'(0)$ can be diagnosed with ADHOC2 (see LR05). Thus, to obtain the total solution for the perturbation pressure, we must determine $p'(0)$ as a function of height.

We can solve for $p'(0)$ if we impose the condition given by Eq. (17). This assumption is equivalent to as-

suming that the area-averaged pressure is close to the base-state pressure. While this is not exactly true, analysis of LES pressure fields for the Wangara case (see LR05) show this to be a good approximation. We can write

$$\frac{\overline{p'}}{\rho} = \frac{1}{\pi R_o^2} \left[\int_0^{(R_i-\varepsilon)} \int_0^{2\pi} p'_i(r) + \int_{(R_i+\varepsilon)}^{R_o} \int_0^{2\pi} p'_o(r) \right] r d\phi dr = 0, \tag{23}$$

where p_i and p_o are the pressures in the inner and outer cylinders, respectively. Substituting from (21) and (22) and integrating, we obtain

$$\begin{aligned}
 p'(0) &= \left(2R_i^2 - \frac{R_i^4}{R_o^2} \right) \left[\frac{3}{16} \left(\frac{\partial w_u}{\partial z} \right)^2 - \frac{B_u}{8} \right] \\
 &- \frac{1}{4} \left(\frac{\partial w_d}{\partial z} \right)^2 \left[\left(3R_i^2 - \frac{R_o^4}{R_i^2} - R_o^2 \right) \ln \frac{R_o}{R_i} + \frac{R_o^2}{R_i^2} (R_o^2 - R_i^2) - \frac{3}{4} \frac{(R_o^4 - R_i^4)}{R_o^2} \right] \\
 &\times \left[\frac{1}{2R_o^2} (R_o^2 - R_i^2) - \ln \frac{R_o}{R_i} \right] \left\{ R_i \left(\frac{\partial p}{\partial r} \right)_{R_i+\varepsilon} + [R_i p_{(R_i+\varepsilon)}] \frac{\partial^2 R_i}{\partial z^2} + 2 \frac{\partial}{\partial z} [R_i p_{(R_i+\varepsilon)}] \frac{\partial R_i}{\partial z} - B_d \frac{R_i^2}{2} \right\} \\
 &- \frac{2}{R_o^2} \left\{ \left[\int_0^{(R_i-\varepsilon)} \frac{\partial^2 \xi_i}{\partial z^2} dr \right] - \int_{(R_i+\varepsilon)}^{R_o} \frac{\partial^2 \xi_o}{\partial z^2} dr \right\} + \frac{2}{R_o^2} \left[\int_{(R_i+\varepsilon)}^{R_o} \left\{ \left(\frac{\partial^2 R_i}{\partial z^2} \right) \left[\frac{1}{R_i} \int_0^{(R_i-\varepsilon)} (rp) dr \right] \right. \right. \\
 &\left. \left. + 2 \left(\frac{\partial R_i}{\partial z} \right) \frac{\partial}{\partial z} \left[\frac{1}{R_i} \int_0^{(R_i-\varepsilon)} (rp) dr \right] \right\} \right],
 \end{aligned} \tag{24}$$

where $\xi_o = \int_0^{(R_i-\varepsilon)} [(1/r) \int_0^r (rp) dr] dr + \int_{(R_i+\varepsilon)}^r [(1/r) \int_{(R_i+\varepsilon)}^r (rp) dr] dr$ and $\xi_i = \int_0^r [(1/r) \int_0^r (rp) dr] dr$.

Equation (24) can be solved for the unknown $p'(0)$. The variables w_u , w_d , B_u , and B_d are known from ADHOC2. We can calculate R_o and R_i as discussed in LR05, and $(\partial p/\partial r)_{R_i+\varepsilon}$ can be calculated using Eq. (A23). The pressure $p_{(R_i+\varepsilon)}$ is known from Eqs. (A8) and (16). Finally, the integral terms can be evaluated directly, while the vertical derivatives of the integrals can be calculated using the finite difference methods discussed in section 2a. A more detailed description of the method used to solve for the pressure in ADHOC2 is given in appendix D.

Figure 2 gives a plot of $p'(0)$ as a function of height for various (height-independent) values of R_o . Here we have used the dry convective boundary layer profiles of w_u , w_d , B_u , B_d , and σ given by Schumann and Moeng (1991) and Young (1988). Figure 2 shows that R_o has a significant effect on both of these constants. ADHOC2 predicts R_o .

a. Solution for the vertical structure

The perturbation pressures in the updraft and downdraft (neglecting other effects such as friction) are represented by Eqs. (21) and (22), respectively. It is important to realize here that the solutions given by Eqs. (21) and (22) are the radial solutions for the pressure at a given height. In order to get the total solution for the pressure; that is, $p(r, z)$, we must solve these equations at every model height. In this section, we describe how we solve for the vertical structure. The terms in Eqs. (21) and (22) that we are discussing here have the form

$$\frac{\partial^2}{\partial z^2} \Pi(r, z), \quad (25)$$

where $\Pi = \int_0^r (1/r) [\int_0^r (rp) dr] dr$ and $\Pi = \int_0^{(R_i-\varepsilon)} (1/r) [\int_0^r (rp) dr] dr + \int_{(R_i+\varepsilon)}^r (1/r) [\int_{(R_i+\varepsilon)}^r (rp) dr] dr$ in Eqs. (21) and (22), respectively. We represent approximate (25) using finite differences; that is,

$$\frac{\partial^2}{\partial z^2} \Pi(r, z) = \frac{(\Pi)_{l+1} - 2(\Pi)_l + (\Pi)_{l-1}}{(\Delta z)^2}, \quad (26)$$

where l is an index denoting a particular level on the vertical grid. The effects of these terms are then incorporated into our solution in the following iterative manner (diagramed in Fig. 3).

1) We solve Eqs. (21) and (22) first by temporarily neglecting all contributions from the terms that involve vertical derivatives. This includes neglecting these contributions in the solution for $p'(0)$ [Eq. (24)] as well.

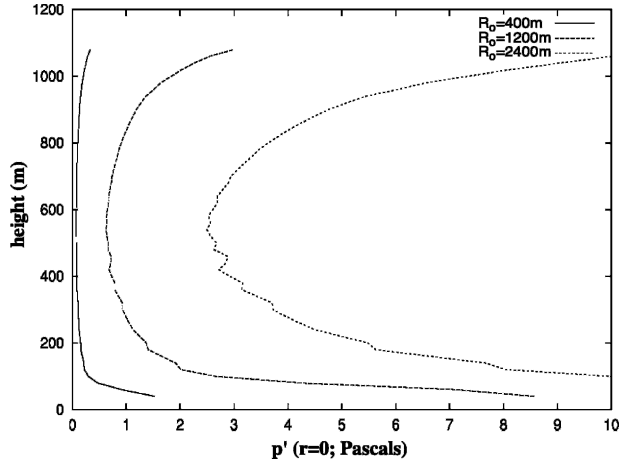


FIG. 2. The pressure at the center of the updraft as a function of height plotted for different values of the updraft radius for the Wangara case.

- 2) We solve for the radial dependence of p that appears in the modified Eqs. (21), (22), and 0.
- 3) Using the solution for p obtained in 2, we approximate the second derivative with respect to z using the centered finite-difference formula given in (26). (We also use finite difference formula for the single z derivative terms.)
- 4) We add the result from step 3 back into Eqs. (21), (22), and (24) and return to step 2. We do this until the solution converges. We find that in practice there is no need to return to step 2.

We note that this representation of the vertical structure is also applied to the ξ_i , ξ_o , and $(\partial^2 R_i/\partial z^2)$ terms in Eq. (24). This algorithm yields $[p'(r)]_i$; that is, an analytical expression for the radial dependence of the perturbation pressure at each finite-difference level.

Finally, we would like to point out that if we also wanted to solve for the radial structure of the pressure using finite difference, we could use a two-dimensional grid relaxation solver. We have used this as a check of the solution algorithm outlined above, with good results.

b. A check on the results so far

To test the model, we used the vertical profiles of w_u , w_d , and R_o given by Schumann and Moeng (1991), as illustrated in their Figs. 3–4 (see also Young 1988). We computed $R_i(z)$ from (1). We calculated the perturbation pressure for day 33 of the Wangara experiments (Hicks 1978), by the method outlined above [this case has been extensively studied by many authors including Wyngaard and Coté (1974), Yamada and Mellor (1975), and André et al. (1978)]. The results are shown in Fig. 4, along with the corresponding LES-derived

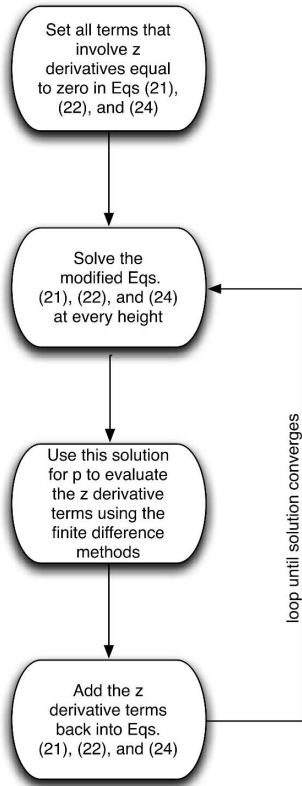


FIG. 3. Flowchart that demonstrates the iteration performed to solve for the perturbation pressure in the clear convective case.

pressure for the Wangara case. For the LES results, we used $R_o = 1100 \text{ m}^{-1}$. This value was obtained by using a composite averaging method similar to what was used by Schumann and Moeng (1991).¹

There is some agreement between the parameterized and LES-derived results. In particular, low pressure is

¹ Centers of updrafts were taken to be grid points where $w' > 2 \text{ m s}^{-1}$ over an entire 1 gridpoint circle surrounding the middle point. Then w' was averaged in concentric circles around each updraft center point and then averaged again over all concentric circles the same distance away from the center points. These averaged values were plotted as a function of distance from the center of the updraft. A clear updraft and downdraft radii emerged from these plots (not shown).

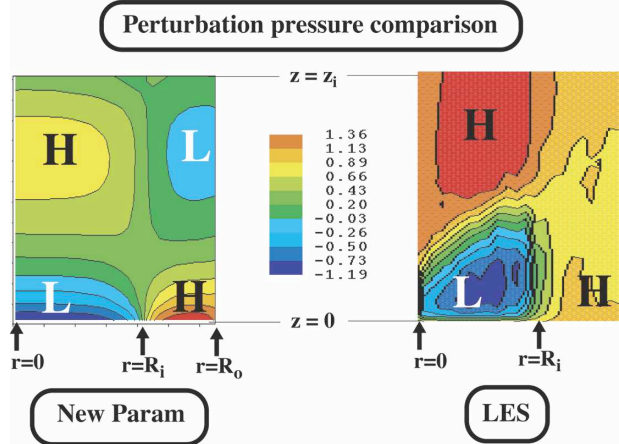


FIG. 4. Comparison of the perturbation pressure (as a function of radius and height) for the new parameterization with that of LES data for the Wangara case. The updraft and downdraft radii are labeled (R_u and R_d , respectively); Z_i is the PBL top height.

found at the updraft center near the surface, and a high pressure is found in the downdraft near the surface; at upper levels, the pressure pattern is reversed. This is what one would expect to find for a clear convective PBL. The strength of the high pressure near the top of the updraft is slightly weaker in the parameterization than the LES. The opposite is true near the surface in the downdraft. These results are encouraging given the sensitivity of $p'(0)$ to the values chosen for R_i (or R_o ; Fig. 2).

c. *Pressure parameterization for use in the $\overline{u'u'}$ and $\overline{w'w'}$ equations*

Recall that our objective is to develop expressions that can be used for the pressure terms in the second-moment momentum equations of our mass-flux model. For the $\overline{u'u'}$ and $\overline{w'w'}$ equations, the expressions that we seek are

$$\frac{\partial}{\partial t} \overline{u'u'} \sim -2 \frac{\overline{u'}}{\rho} \frac{\partial p}{\partial x} \quad \text{and} \quad \frac{\partial}{\partial t} \overline{w'w'} \sim -2 \frac{\overline{w'}}{\rho} \frac{\partial p}{\partial z}. \quad (27)$$

We can write the right-hand side (rhs) of the $\overline{u'u'}$ equation in (27) as

$$2 \frac{\overline{u'}}{\rho} \frac{\partial p}{\partial x} = 2 \frac{\overline{U'}}{\rho} \frac{\partial p}{\partial r} \cos^2 \phi = \frac{2}{\pi R_o^2} \left(\int_0^{R_i} \int_0^{2\pi} \frac{U'}{\rho} \frac{\partial p}{\partial r} + \int_{R_i}^{R_o} \int_0^{2\pi} \frac{U'}{\rho} \frac{\partial p}{\partial r} \right) \cos^2 \phi \, d\phi \, dr, \quad (28)$$

where ϕ is the angle between the radial vector and the x axis and U' is the total perturbation wind vector.

Integrating this equation gives (the details of this are given in appendix B).

$$\begin{aligned}
\frac{\overline{u' \partial p}}{\rho \partial x} = & \frac{1}{R_o^2} \left\{ \frac{-R_i^4}{16} \left(\frac{\partial w_u}{\partial z} \right) \left[B_u - \frac{3}{2} \left(\frac{\partial w_u}{\partial z} \right)^2 \right] + \frac{R_i}{2\rho} \left(\frac{\partial w_d}{\partial z} \right) \left(\frac{\partial p}{\partial r} \right)_{R_i+\varepsilon} \left(R_o^2 \ln \frac{R_o}{R_i} - \frac{R_o^2 - R_i^2}{2} \right) \right\} \\
& + \frac{1}{8R_o^2} \left(\frac{\partial w_d}{\partial z} \right)^3 \left[\left(\frac{R_o^6}{R_i^2} - \frac{7R_o^4}{4} + \frac{3R_i^4}{4} \right) - \left(\frac{R_o^6}{R_i^2} - 3R_o^2 R_i^2 + R_o^4 \right) \ln \frac{R_o}{R_i} \right] + \frac{B_d}{16R_o^2} \left(\frac{\partial w_d}{\partial z} \right) [R_o^4 - R_i^4] \\
& + \frac{1}{R_o^2} \left\{ \int_0^{R_i} \frac{r}{2} \left(\frac{\partial w_u}{\partial z} \right) \left[\int_0^r r \frac{\partial^2}{\partial z^2} \left(\frac{p}{\rho} \right) dr \right] dr \right\} + \frac{1}{R_o^2} \left\{ \int_{R_i}^{R_o} \frac{(r^2 - R_o^2)}{2} \left(\frac{\partial w_d}{\partial z} \right) \left[\int_{(R_i+\varepsilon)}^r r \frac{\partial^2}{\partial z^2} \left(\frac{p}{\rho} \right) dr \right] dr \right\}.
\end{aligned} \tag{29}$$

In (29),

$$\frac{\overline{u' \partial p}}{\rho \partial x} = f \left[B_u, B_d, R_i, R_o, \frac{\partial w_u}{\partial z}, \frac{\partial w_d}{\partial z}, \left(\frac{\partial p}{\partial r} \right)_{R_i+\varepsilon} \right]. \tag{30}$$

We can calculate $(\partial p / \partial r)_{R_i+\varepsilon}$ from (A23). If we assume that \overline{B} and \overline{w} are equal to zero, and that R_i can be determined from R_o [using the updraft area fraction, σ and Eq. (1)], we can write

$$\frac{\overline{u' \partial p}}{\rho \partial x} = f \left(B_u, R_i, \frac{\partial w_u}{\partial z} \right). \tag{31}$$

Thus, if we know B_u , R_i , and $\partial w_u / \partial z$, we can solve for the pressure contribution in the $\overline{u' u'}$ equation. ADHOC2 determines all three of these quantities (see LR01a and LR05).

As discussed, ADHOC1 uses standard second-order closure parameterizations for the pressure terms. To see if the new parameterization (29) makes a difference, we ran ADHOC2 3 times for day 33 of the Wangara experiment—twice with conventional pressure parameterizations (given by R51 and L75/ZL79, respectively), and once with Eq. (29). In the third run, we used the prescribed profile of R_i from Schumann and Moeng (1991, their Fig. 4). We also simulated the same case using a large-eddy simulation model (Khairoutdinov and Randall 2003). The results from all four simulations are shown in Figs. 5–6.

Fig. 5 shows the evolution of $-\overline{u' \partial p' / \partial x}$ in height and time for each of these cases. The run that used Eq. (29) (Fig. 5a) exhibits the best agreement with $-\overline{u' \partial p' / \partial x}$ as diagnosed from the LES results (Fig. 5d). Although it increases faster than the LES as the PBL starts to grow, it tapers off at the end of the simulation [~ 6 P.M. local time (LT)] in a manner very similar to the LES. The maximum height of the pressure effects extends to approximately 1700 m for both the LES and the ADHOC run that used Eq. (29). The runs that used R51 and L75/ZL79 show a delayed pressure response to the sur-

face heating as well as a delayed response to the setting of the sun in the late afternoon. The pressure effects in the PBL do not get above 1300 m (which is the PBL top) in these runs. The reason for the latter difference may very well relate to prescription of the turbulent length scale, which is required in the R51 and L75/ZL79 parameterizations. This length scale gets very small near the PBL top, and so the dissipation of the momentum variances becomes very efficient. When the energy near the PBL top is dissipated, the pressure terms go to zero.

Figure 6 shows a cross section through the contours plotted in Fig. 5 at hour 13 (1 P.M. LT). The shapes and magnitudes of the LES and new parameterization profiles are very similar, with the greatest differences near the surface and near the inversion. The parameterized values actually become slightly negative in the inversion layer. We can compare our results to Mason's (1989). His Fig. 15 shows $-\overline{u' \partial p' / \partial x}$ for an idealized convective PBL. The shape and magnitude are very similar to what is seen here—fairly constant and positive in the bulk of the PBL, with an increase near the surface. However, they also show a small increase near the inversion layer. This is not seen for Wangara (the parameterization shows a slight decrease while the LES shows no change). The differences may be due to the facts that the vertical resolution in the Mason run was twice that used here and the inversion was slightly stronger. A double resolution run with the current LES (not shown) produces a slight increase near the inversion, although it is much smaller than that obtained by Mason (1989). The R51 + L75/ZL79 curve does a nice job in the lower part of the PBL. However, it goes to zero 800 m below the LES and gets very large near the surface.

In general, we would expect $-\overline{u' \partial p' / \partial x}$ to be positive near the surface, because this implies low pressure in the updraft near the surface. In a dry convective boundary layer, this low pressure results from surface heating and is the mechanism by which air is drawn into the

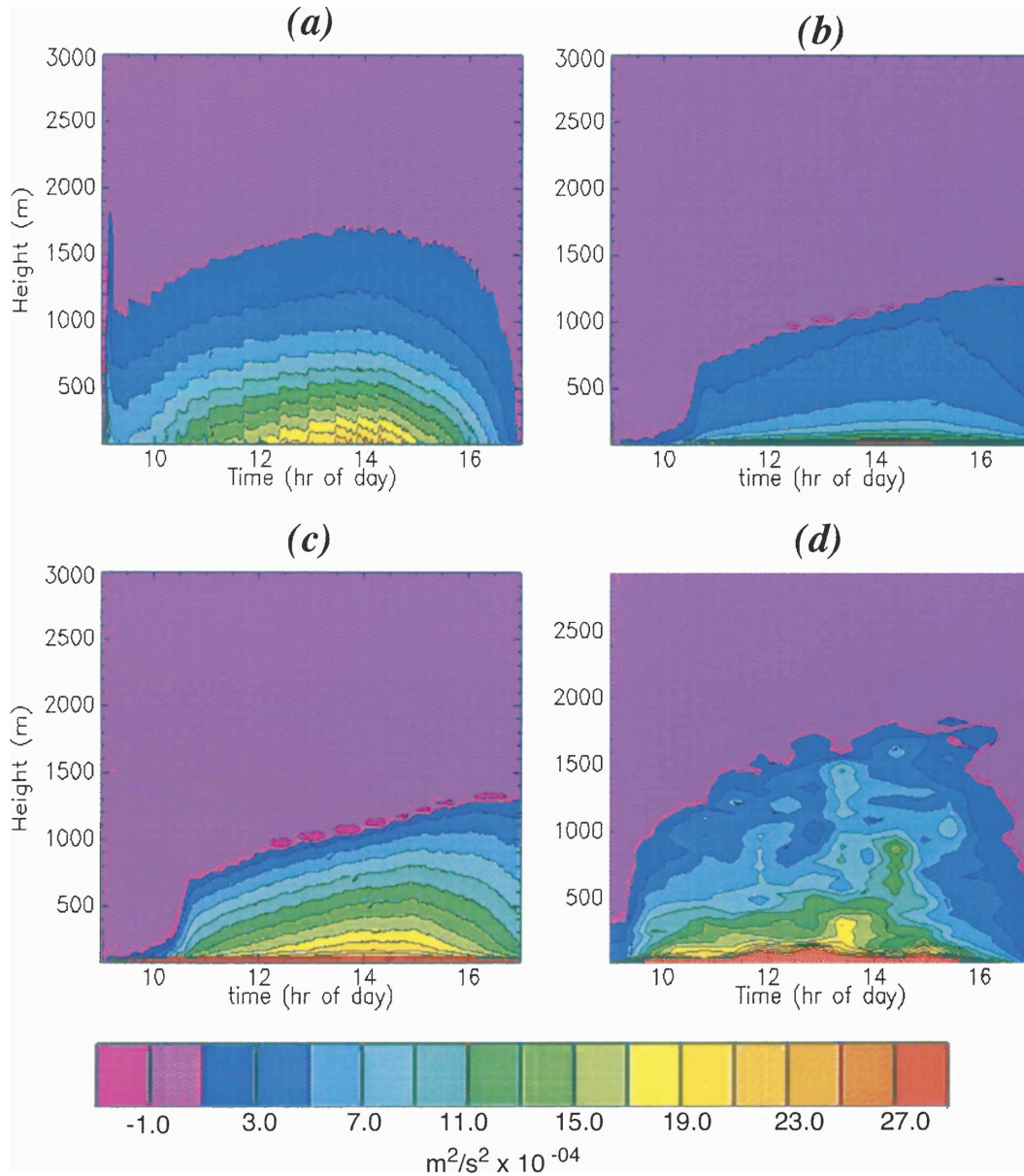


FIG. 5. Comparison of the evolution of $-\overline{u'\partial p'/\partial x}$ over the first 8 h of the Wangara simulation for (a) the new parameterization given by Eq. (29), (b) the Rotta parameterization, (c) the Rotta plus Launder parameterization, and (d) LES.

updraft. However, using similar reasoning, we would expect $-\overline{u'\partial p'/\partial x}$ to be positive up high. This is not the case for the parameterization, but is the case in the results of Mason (1989) and in the LES. The parameterization does not perform as well near the inversion as it does in the rest of the boundary layer. A similar analysis was performed for the pressure term in the $\overline{w'w'}$ equation ($-\overline{w'\partial p'/\partial z}$); it provided no new insight.

Until now, we have focused on the actual pressure term that appears in the equations for $\overline{u'u'}$ and $\overline{w'w'}$

($-\overline{u'\partial p'/\partial x}$ and $-\overline{w'\partial p'/\partial z}$, respectively). However, as discussed earlier, these terms are not the ones modeled in higher-order closure models. Typically these terms are divided into pressure diffusion terms ($-\overline{\partial u'p'/\partial x}$ and $-\overline{\partial w'p'/\partial z}$) and return-to-isotropy terms ($\overline{p'\partial u'/\partial x}$ and $\overline{p'\partial w'/\partial z}$). The pressure-diffusion term is either neglected or lumped together with the transport (triple moment) term, while the return-to-isotropy term is parameterized using either R51 or L75/ZL79. Thus, in Fig. 7, we show the R51 and L75/ZL79 parameteriza-

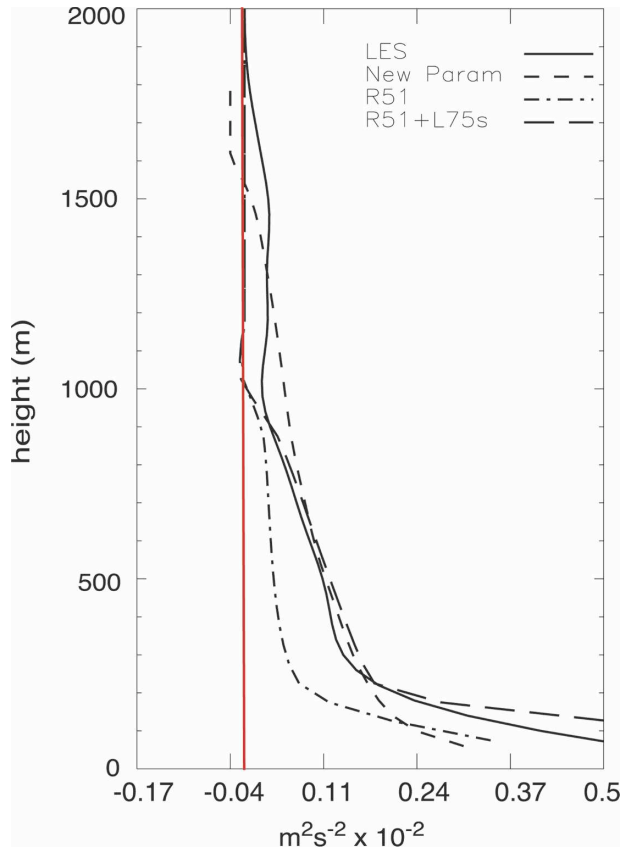


FIG. 6. Comparison of $-\overline{u'w'}/\partial x$ calculated with the new parameterization given by Eq. (29) (short dashed), the Rotta parameterization (dashed-dotted), the Rotta plus Launder parameterization (long dashed), and LES (solid) for the Wangara case at hour 13 (1 P.M. LT). The red line is the zero line.

tions (and their sum) for the return-to-isotropy terms in the $\overline{u'u'}$ and $\overline{w'w'}$ equations. We also show a relatively new parameterization, which improved R51 and L75/ZL79, developed by Cheng et al. (2002), along with the LES-derived values and the new parameterization results. The best agreement with the LES is obtained with the new parameterization for both $\overline{p'\partial u'/\partial x}$ and $\overline{p'\partial w'/\partial z}$. The latter is particularly striking. The next best agreement is with Cheng et al. (2002) parameterization—the only other one that is able to get the correct sign of the term throughout the PBL). The R51 results for $\overline{p'\partial u'/\partial x}$ are too large in the lower half of the PBL and too small in the upper half. L75/ZL79 brings R51 closer to the LES, but the differences are still large, especially near the inversion where the R51 plus L75/ZL79 parameterization gives the wrong sign. A very similarly shaped curve for the R51 parameterization in the $\overline{w'w'}$ equation was found by Deardorff (1974, their Fig. 20) in their simulation of the same Wangara, day 33 case.

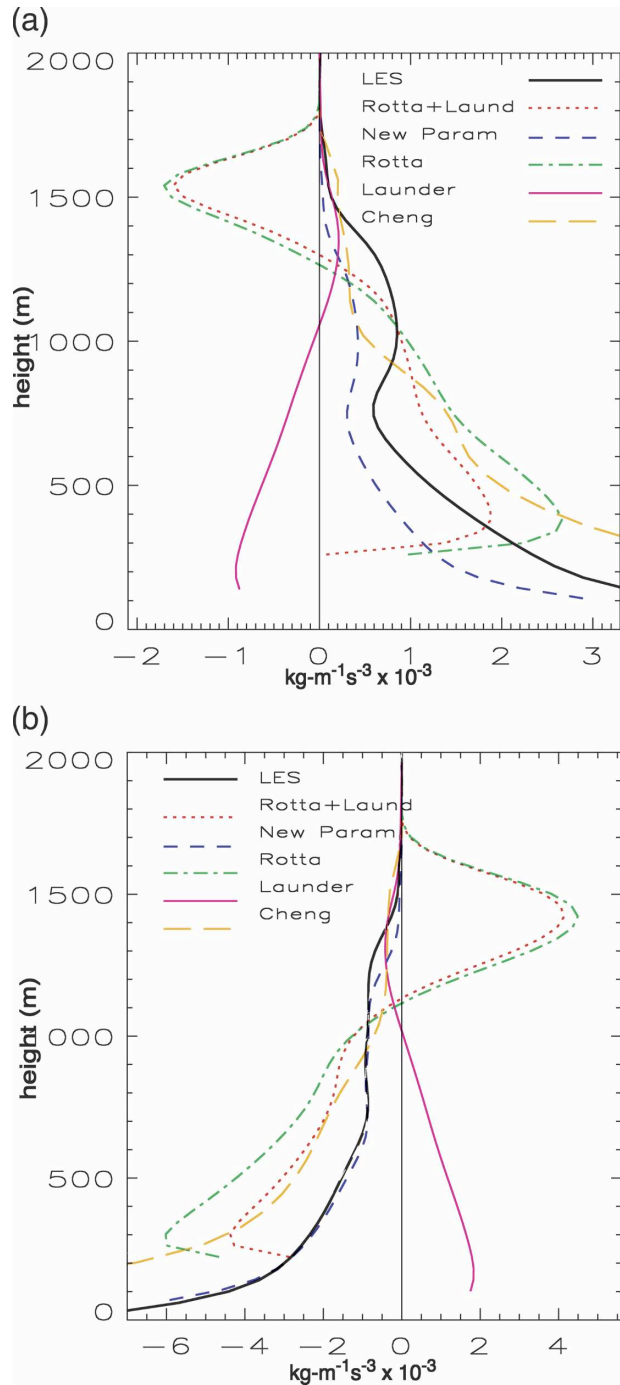


FIG. 7. Here, (a) $\overline{p'\partial u'/\partial x}$ and (b) $\overline{p'\partial w'/\partial z}$ are calculated with the new parameterization, the R51, L75, and Cheng et al. (2002) parameterizations (with the terms calculated using LES data), and the LES data for the Wangara case.

3. Rolls

To represent rolls, we use a series of alternating updrafts and downdrafts (Fig. 1b). The width of an updraft (downdraft) is denoted by L_u (L_d) and the total width of the roll is $L = L_u + L_d$, where

$$L_u \equiv x_1 - x_0 \quad \text{and} \quad L_d \equiv x_2 - x_1. \quad (32)$$

We let L_u and L_d vary with height, but the total roll width L is assumed to be independent of height; that is,

$$\frac{\partial L}{\partial z} = 0. \quad (33)$$

The updraft and downdraft fractional areas are (respectively)

$$\sigma = L_u/L \quad \text{and} \quad 1 - \sigma = L_d/L. \quad (34)$$

One key to accurately representing the pressure–velocity correlations in such a roll is to know its aspect ratio, a (the width divided by the height). Previous studies of rolls show that the aspect ratio depends on a bulk Richardson number, or alternatively, on the ratio of the PBL height to the Monin–Obukhov length, z_i/L_{MO} (Deardorff 1972; Moeng and Sullivan 1994; Glendening 1996; Sykes and Henn 1988; Chou and Ferguson 1991). Most of the studies agree that rolls are found for $-1.5 \leq z_i/L_{MO} \leq -10$ with aspect ratios in the range $2 \leq a \leq 15$. The case we will examine here is that of Glendening (1996, hereafter G96). In the G96 case, $z_i/L_{MO} = -2.5$ and $a = 4$. For a discussion of our G96 case, see LR05.

We simulated the G96 case with the LES model described by Khairoutdinov and Randall (2003). We adopt a Cartesian coordinate system, with the y axis parallel to the mean wind. Figure 8 shows an x – y and an x – z cross section of the LES perturbation vertical velocity for this run. The roll structures are apparent in both plots. The white squares indicate the regions that we have classified as rolls. Only the data from these squares have been used in our analysis.

Rolls are observed to have an orientation ranging from -20° to $+30^\circ$ relative to the mean wind (Moeng and Sullivan 1994). To determine the orientation of the rolls in the G96 LES run, we used an autocorrelation method similar to what we used to determine R_o in the clear convective case. We found the autocorrelation in the LES data for lines across the domain that whose angles with the y axis (the axis of mean wind) ranged from -15° to 15° . The highest correlation was found for lines with an angle of 8° to the left of the mean wind. Figure 8 supports this value. This implies modest rates of change in the y direction (perpendicular to the page in Fig. 1b). However, for simplicity here, we assume that the orientation angle is 0° , so that we can neglect terms involving $\partial/\partial y$.

Solution for the perturbation pressure

Using Cartesian coordinates for this case, the Boussinesq continuity equation is

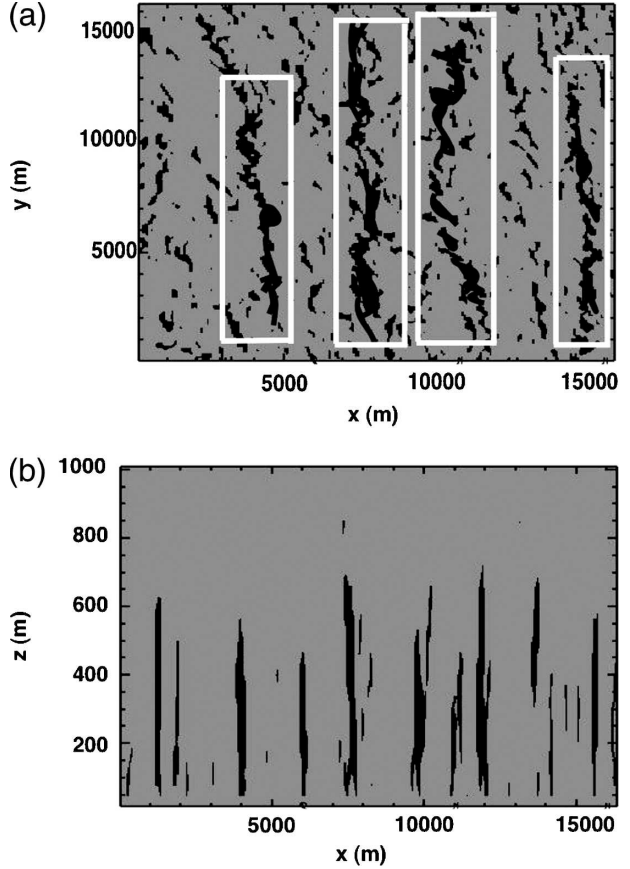


FIG. 8. Perturbation vertical velocity for the LES roll case simulation: (a) x – y cross section through the PBL center and (b) x – z cross section at the midpoint in y . Values of w' greater than 0.5 m s^{-1} are black. The white squares in (a) indicate the regions classified as rolls in this paper.

$$\frac{\partial u}{\partial x} + \frac{\partial w}{\partial z} = 0. \quad (35)$$

In the updraft (downdraft) $w = w_u$ ($w = w_d$) uniformly (see Fig. 1b). We integrate Eq. (35) in x separately over the updraft and downdraft to determine $u(x)$. The results are:

$$u(x) = u(x_0 + \varepsilon) - (x - x_0) \frac{\partial w_u}{\partial z} \quad \text{for} \quad x_0 < x < x_1 \quad (36)$$

and

$$u(x) = u(x_0 + \varepsilon) - L_u \frac{\partial w_u}{\partial z} - (w_u - w_d) \frac{\partial x_1}{\partial z} - (x - x_1) \frac{\partial w_d}{\partial z} \quad \text{for} \quad x_1 < x < x_2. \quad (37)$$

Neglecting rotation and friction, and using the assumption $(\partial/\partial y) = 0$, the equations of horizontal and vertical motion in Cartesian coordinates can be written as

$$\frac{\partial u}{\partial t} + u \frac{\partial u}{\partial x} + w \frac{\partial u}{\partial z} = - \frac{\partial}{\partial x} \left(\frac{p'}{\rho} \right) \quad (38)$$

and

$$\frac{\partial w}{\partial t} + u \frac{\partial w}{\partial x} + w \frac{\partial w}{\partial z} = - \frac{\partial}{\partial z} \left(\frac{p'}{\rho} \right) + g \frac{\theta'_v}{\theta_0}, \quad (39)$$

respectively. Taking $(\partial/\partial x)$ of (38) and $(\partial/\partial z)$ of (39), adding the results, and rearranging, we obtain

$$\frac{\partial^2}{\partial x^2} \left(\frac{p'}{\rho} \right) + \frac{\partial^2}{\partial z^2} \left(\frac{p'}{\rho} \right) = -2 \left[\left(\frac{\partial w}{\partial x} \frac{\partial u}{\partial z} \right) + \left(\frac{\partial w}{\partial z} \right)^2 \right] + B, \quad (40)$$

where B is defined by (11).

The vertical boundary conditions are (18)–(19). The horizontal conditions are Eq. (17) and that the rolls are periodic. It also must be true that p' is continuous everywhere. To solve (40) subject to these conditions, we use an analytical method to determine the horizontal structure, and a finite-difference method to determine the vertical structure. This idea behind doing this is explained in section 2. We begin by integrating Eq. (40) in x separately for the updraft and downdraft regions, using the expressions given by (36) and (37) for $u(x)$. We also use our assumption that the vertical velocity and potential temperature are horizontally uniform within the updraft and the downdraft.

As shown in appendix C, the solutions are

$$\frac{p'}{\rho} = \left(\frac{p'}{\rho} \right)_{x_0+\varepsilon} + (x - x_0) \left[\frac{\partial}{\partial x} \left(\frac{p'}{\rho} \right) \right]_{x_0+\varepsilon} + \frac{(x - x_0)^2}{2} \left[-2 \left(\frac{\partial w_u}{\partial z} \right)^2 + B_u \right] - \int_{(x_0+\varepsilon)}^x \left[\int_{(x_0+\varepsilon)}^x \frac{\partial^2}{\partial z^2} \left(\frac{p'}{\rho} \right) dx \right] dx$$

for $x_0 < x < x_1$. (41)

and

$$\frac{p'}{\rho} = \left(\frac{p'}{\rho} \right)_{x_0+\varepsilon} + L_u \left[\frac{\partial}{\partial x} \left(\frac{p'}{\rho} \right) \right]_{x_0+\varepsilon} + \frac{L_u^2}{2} \left[-2 \left(\frac{\partial w_u}{\partial z} \right)^2 + B_u \right] - \int_{(x_0+\varepsilon)}^{(x_1-\varepsilon)} \left[\int_{(x_0+\varepsilon)}^x \frac{\partial^2}{\partial z^2} \left(\frac{p'}{\rho} \right) dx \right] dx$$

$$+ (x - x_1) \left[\frac{\partial}{\partial x} \left(\frac{p'}{\rho} \right) \right]_{x_1+\varepsilon} + \frac{(x - x_1)^2}{2} \left[-2 \left(\frac{\partial w_d}{\partial z} \right)^2 + B_d \right] - \int_{(x_1+\varepsilon)}^x \left[\int_{(x_1+\varepsilon)}^x \frac{\partial^2}{\partial z^2} \left(\frac{p'}{\rho} \right) dx \right] dx$$

for $x_1 < x < x_2$. (42)

At the updraft–downdraft borders (i.e., $x = x_0$ and $x = x_1$), there is no contribution to the pressure terms because p is continuous there. However, $(\partial/\partial x)p'$ can be discontinuous at these borders.

Equations (41)–(42) contain the unknowns $[(\partial/\partial x)(p'/\rho)]_{x_0+\varepsilon}$, $[(\partial/\partial x)(p'/\rho)]_{x_1+\varepsilon}$ and $(p'/\rho)_{x_0+\varepsilon}$. Appendix C describes how to solve for these. The only variables needed as input are the updraft and downdraft vertical velocities and potential temperatures (which are known from ADHOC), and the values of L_u and L_d (which are calculated using the methods discussed in LR05). The solution for the vertical structure of the pressure is obtained using finite-difference methods, as described in section 2a. A detailed description of how to solve for the pressure (in ADHOC2) in the axisymmetric case is given in appendix D. The solution method for this roll case is solved analogously.

To test our parameterization, we use the LES described by Khairoutdinov and Randall (2003) to simulate the case described by G96. We get the profiles of w_u and w_d from the LES data (using data from the white boxes in Fig. 8). We then use Eqs. (36)–(37) to get the profiles of $u(x)$ at each height (here, we use the value of L_u calculated in LR05). We use these velocities and the LES-derived values of θ'_v in Eqs. (41)–(42) and use the methods outlined above to get the pressure fields. These fields are then averaged appropriately to get the pressure–velocity gradient covariance terms that appear in the second-moment flux equations (calculated as in section 2c). These averages are taken over the entire LES domain. We compare these results to those obtained with the LES and the parameterizations of R51 and L75/ZL79 for this case. As discussed earlier, the actual pressure term in the momentum flux and

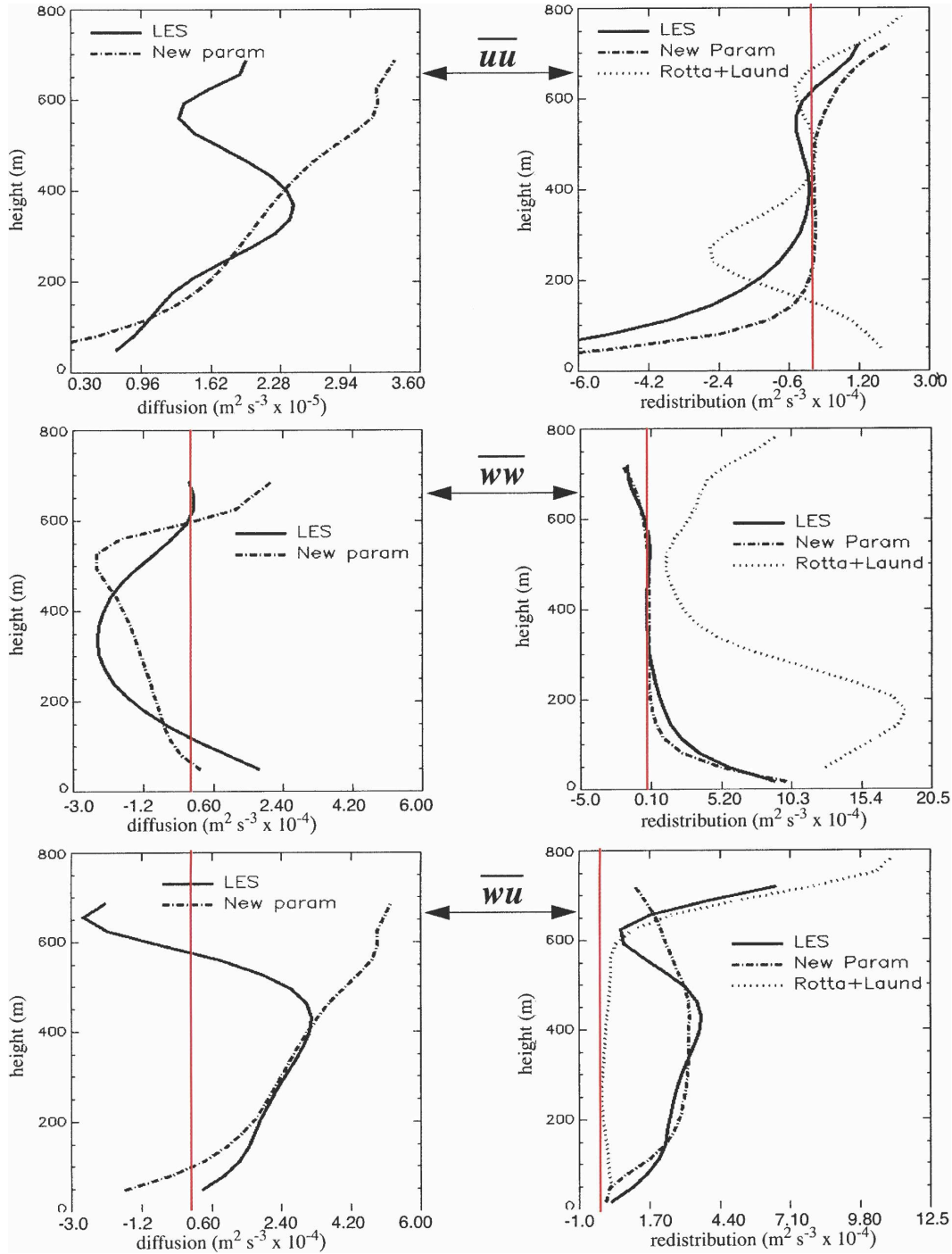


FIG. 9. A comparison of LES, parameterized, and R51 plus L75 values for (left) the pressure diffusion and (right) the pressure return-to-isotropy in the (top) $\overline{u'u'}$, (middle) $\overline{w'w'}$, and (bottom) $\overline{w'u'}$ equations. The red lines are the zero lines.

variance equations is often separated into a pressure diffusion and return-to-isotropy terms. In Fig. 9, we compare the LES-derived values for both the return-to-isotropy and the diffusion terms to our parameter-

ized values for the $\overline{u'u'}$, $\overline{w'w'}$, and $\overline{w'u'}$ equations. For the return-to-isotropy term, we also include a plot of the R51 plus L75/ZL79 parameterization. The three plots in the left-hand column are profiles of the pres-

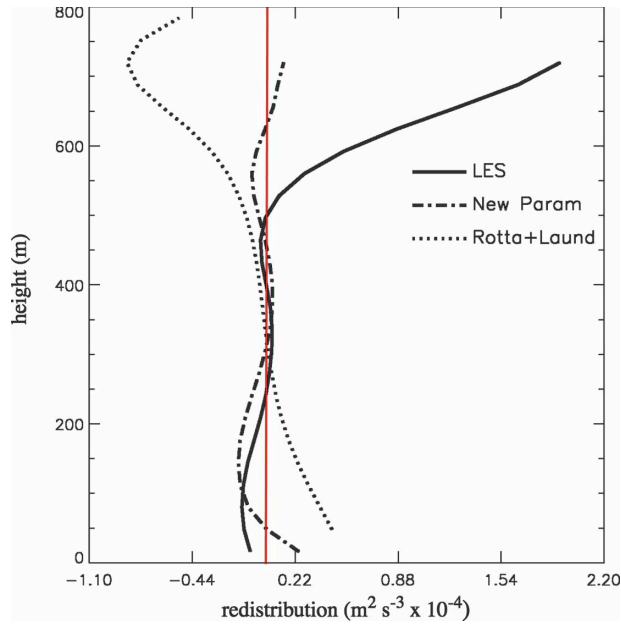


FIG. 10. A comparison of LES, parameterized, and R51 and L75 values for the pressure return-to-isotropy in the $\overline{w'T}$ equation. The red line is the zero line.

sure diffusion term, while the three plots in the right-hand column show profiles of the return-to-isotropy term. Figure 10 compares the return-to-isotropy term in the heat flux ($\overline{w'T}$) equation.

We have obtained very nice agreement between the LES and our parameterization for the return-to-isotropy term, especially in the two variance equations. In the $\overline{w'u'}$ and $\overline{w'T}$ equations, there are some differences up high near the inversion. In Fig. 10, the R51 + L75 and the new parameterizations show a slight positive value close to the surface, while the literature support negative values here (e.g., Wyngaard and Coté 1971). The R51 plus L75/ZL79 parameterization does a reasonable job in the $\overline{u'u'}$ equation except in the lower quarter of the PBL. However, it does not handle the $\overline{w'w'}$ return-to-isotropy term well. For the $\overline{w'u'}$ return-to-isotropy term, it does an excellent job in the upper PBL, but performs poorly down low. The disagreement between the R51 plus L75/ZL79 parameterization and the LES can likely be attributed to the calculation of the turbulent length scale and the choice of constants. In this simulation, we have calculated the length scale using Bougeault and André (1986) and used the constants listed in the original L75 papers. While there is disagreement about the optimal choice for these length scales and constants, changing their values should mostly affect the magnitude of the curves (the shape of the curve will be affected in a minimal way as the relative importance of the R51 and L75/ZL79 terms

changes with the choice of constants). Tuning the length scale and choice of constants to fit the LES curves may make the R51 plus L75/ZL79 agreement closer in the $\overline{w'u'}$ and $\overline{w'w'}$ equations. However, it will not help the lower half of the $\overline{u'u'}$ equation, which clearly has the wrong shape. In any case, tuning constants to fit data is not an optimal approach.

In the left-hand columns of Fig. 9, we compare the LES diffusion term to that of the new parameterization.² The agreement is very good in the lower $\frac{2}{3}$ of the PBL. Near the inversion, the parameterization does not perform very well, except in the $\overline{w'w'}$ equation. Since this problem does not manifest itself in the return-to-isotropy plots, it is likely related to the difference in the slope of the pressure profile (the return-to-isotropy term does not involve derivatives of the pressure). Despite the reason for the disagreement, it is pretty clear that the pressure diffusion term is not negligible for this case. It is the same order of magnitude as the return-to-isotropy term in the $\overline{w'w'}$ and $\overline{w'u'}$ equations. The studies of Wyngaard and Coté (1971) and McBean and Elliot (1975) support the importance of this term.

4. Discussion

In this paper, we have described a simple new way to represent the pressure terms in PBL mass-flux models. This method requires no specific tuning of parameters. The new parameterization is based on the assumption that coherent structures dominate the PBL physics. We idealize the geometry of these structures and diagnose the perturbation pressure. We have considered two geometries: plumes (Wangara, day 33; André et al. 1978) and rolls (Glendening 1996). We simulated both cases using the LES model of Khairoutdinov and Randall (2003). In both cases, our simple geometrically based parameterization allowed us to represent the pressure terms in the Reynolds stress equations more accurately than the standard parameterizations of R51 and L75/ZL79. The closest agreement to standard parameterizations was found for the Cheng et al. (2002). For the cases analyzed here, the pressure-diffusion term is not negligible. This supports the conclusions of Wyngaard and Coté (1971) and McBean and Elliot (1975).

² We note here that the diffusion term in the $\overline{u'u'}$ equation is given by $\partial(\overline{p'u'})/\partial x$, which should be identically zero if averaged horizontally over the LES domain. In Fig. 9, it is not equal to zero. This is because the averaging was done over the roll structure (indicated by the white boxes in Fig. 8) and not, over the whole LES domain. However, it is small (an order of magnitude smaller than the same term in $\overline{w'w'}$ equation).

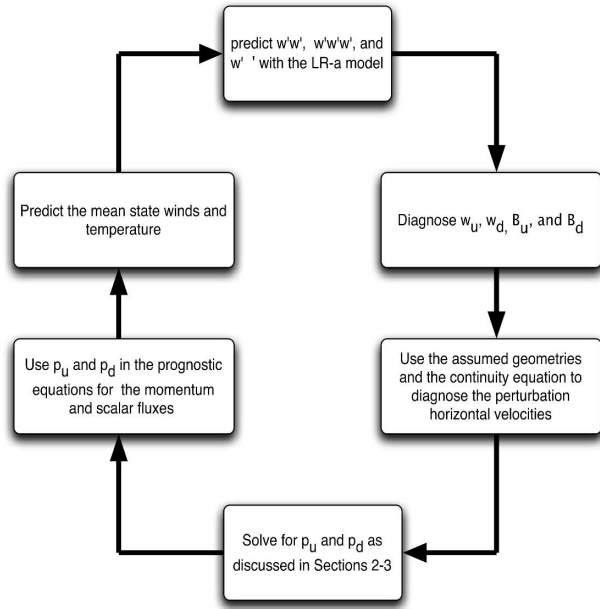


FIG. 11. Method of implementation of the new pressure parameterization in the LR01a/LR05 model.

Figure 11 summarizes our approach with a flowchart. The parameterization requires the values of w_u , w_d , B_u , and B_d [as defined in Eq. (20)] that are diagnosed in the mass-flux model. The plume geometry requires two additional variables (either R_u or R_d) and σ . The latter is also diagnosed in the ADHOC model. The former is calculated as discussed in LR05.

For the Wangara case the Richardson number (Ri) is large and positive, while for the G96 case it is negative. For intermediate cases, a simple interpolation based on Ri may provide a good estimate of the pressure terms. This idea will be explored in future work.

Acknowledgments. This research was funded by the National Science Foundation under Grant ATM-9812384, by the U.S. Department of Energy under Cooperative Agreement DE-FC02-01ER63163, both to Colorado State University, and by the National Oceanic and Atmospheric Administration under Grant NA17RJ1228.

APPENDIX A

Radial Solution for the Perturbation Pressure in the Axisymmetric Case

a. Inner cylinder

Equation (10) is rewritten here as

$$\frac{\partial}{\partial r} \left[r \frac{\partial}{\partial r} \left(\frac{p'}{\rho} \right) \right] + r \frac{\partial^2}{\partial z^2} \left(\frac{p'}{\rho} \right) = -r \left[\left(\frac{\partial v_r}{\partial r} \right)^2 + 2 \frac{\partial w}{\partial r} \frac{\partial v_r}{\partial z} + \left(\frac{\partial w}{\partial z} \right)^2 + \left(\frac{v_r}{r} \right)^2 \right] + rB. \quad (A1)$$

Within the inner cylinder, $(\partial w / \partial r) = 0$ so that second term on the rhs of (A1) vanishes. Using Eq. (4) and its radial derivative, we can rewrite Eq. (A1) for the inner cylinder as

$$\frac{\partial}{\partial r} \left[r \frac{\partial}{\partial r} \left(\frac{p'}{\rho} \right) \right] = rB_u - \frac{3r}{2} \left(\frac{\partial w_u}{\partial z} \right)^2 - r \frac{\partial^2}{\partial z^2} \left(\frac{p'}{\rho} \right) \quad \text{for } r < R_i. \quad (A2)$$

Here, B_u is defined by Eq. (20), and is independent of r . We integrate (A2) from $r = 0$ to $r = r$, and use boundary condition (14) to get

$$\frac{\partial}{\partial r} \left(\frac{p'}{\rho} \right) = \frac{r}{2} \left[B_u - \frac{3}{2} \left(\frac{\partial w_u}{\partial z} \right)^2 \right] - \frac{1}{r} \int_0^r \left[r \frac{\partial^2}{\partial z^2} \left(\frac{p'}{\rho} \right) \right] dr \quad \text{for } r < R_i. \quad (A3)$$

Further integration of (A3) from $r = 0$ to $r = r$ gives

$$\frac{p'(r)}{\rho} = \frac{p'(0)}{\rho} + B_u \left(\frac{r^2}{4} \right) - \frac{3r^2}{8} \left(\frac{\partial w_u}{\partial z} \right)^2 - \int_0^r \left\{ \frac{1}{r} \int_0^r \left[r \frac{\partial^2}{\partial z^2} \left(\frac{p'}{\rho} \right) \right] dr \right\} dr \quad \text{for } r \leq R_i, \quad (A4)$$

which can be rewritten as

$$\frac{p'(r)}{\rho} = \frac{p'(0)}{\rho} + B_u \left(\frac{r^2}{4} \right) - \frac{3r^2}{8} \left(\frac{\partial w_u}{\partial z} \right)^2 - \frac{\partial^2}{\partial z^2} \left\{ \int_0^r \left[\frac{1}{r} \int_0^r (rp') dr \right] dr \right\} \quad \text{for } r \leq R_i. \quad (A5)$$

Note that $p'(0)$ is unknown at this stage. As special cases of (A3) and (A4), we have, respectively,

$$\left[\frac{\partial}{\partial r} \left(\frac{p'}{\rho} \right) \right]_{R_i - \varepsilon} = \frac{R_i}{2} \left[B_u - \frac{3}{2} \left(\frac{\partial w_u}{\partial z} \right)^2 \right] - \frac{1}{R_i} \int_0^{R_i - \varepsilon} \left[r \frac{\partial^2}{\partial z^2} \left(\frac{p'}{\rho} \right) \right] dr \quad (\text{A6})$$

and

$$\frac{p'(R_i - \varepsilon)}{\rho} = \frac{p'(0)}{\rho} + \left(\frac{R_i^2}{4} \right) \left[B_u - \frac{3}{2} \left(\frac{\partial w_u}{\partial z} \right)^2 \right] - \int_0^{R_i - \varepsilon} \left\{ \frac{1}{r} \int_0^r \left[r \frac{\partial^2}{\partial z^2} \left(\frac{p'}{\rho} \right) \right] dr \right\} dr. \quad (\text{A7})$$

Using Leibniz's rule, we can pull the z derivatives out of the integral in (A7) and write

$$\frac{p'(R_i - \varepsilon)}{\rho} = \frac{p'(0)}{\rho} + \left(\frac{R_i^2}{4} \right) \left[B_u - \frac{3}{2} \left(\frac{\partial w_u}{\partial z} \right)^2 \right] - \frac{\partial^2}{\partial z^2} \left\{ \int_0^{(R_i - \varepsilon)} \frac{1}{r} \left[\int_0^r (rp) dr \right] dr \right\} - \left(\frac{\partial^2 R_i}{\partial z^2} \right) \left[\frac{1}{R_i} \int_0^{(R_i - \varepsilon)} (rp) dr \right] - 2 \left(\frac{\partial R_i}{\partial z} \right) \frac{\partial}{\partial z} \left[\frac{1}{R_i} \int_0^{(R_i - \varepsilon)} (rp) dr \right]. \quad (\text{A8})$$

We use the form given by (A8) as opposed to that given by (A7) because (A8) is easier to evaluate in the context of a finite difference model such as ADHOC2.

b. Updraft–downdraft boundary

Now consider the boundary at $r = R_i$, where both w and v_r are, in general, discontinuous. As noted in Eq. (16), the pressure must be continuous across this boundary. The radial pressure gradient can be discontinuous, however.

We begin by rewriting Eq. (3) as

$$\frac{\partial v_r}{\partial r} + \frac{v_r}{r} = - \frac{\partial w}{\partial z}. \quad (\text{A9})$$

Square both sides of (A9), and rearranging gives

$$\left(\frac{\partial v_r}{\partial r} \right)^2 + \left(\frac{v_r}{r} \right)^2 = \left(\frac{\partial w}{\partial z} \right)^2 + 2 \frac{v_r}{r} \left(\frac{\partial w}{\partial z} + \frac{v_r}{r} \right). \quad (\text{A10})$$

Substitute this into (A1) to obtain

$$\frac{\partial}{\partial r} \left[r \frac{\partial}{\partial r} \left(\frac{p'}{\rho} \right) \right] + r \frac{\partial^2}{\partial z^2} \left(\frac{p'}{\rho} \right) = -2 \left[r \frac{\partial w}{\partial r} \frac{\partial v_r}{\partial z} + r \left(\frac{\partial w}{\partial z} \right)^2 + v_r \left(\frac{\partial w}{\partial z} + \frac{v_r}{r} \right) \right] + r \frac{g}{\theta_0} \frac{\partial \theta'_v}{\partial z}. \quad (\text{A11})$$

It is not straightforward to radially integrate (A11) across $r = R_i$ because the first two terms on the rhs involve products of quantities that “go to infinity” there. To proceed, we use a coordinate transformation as follows:

$$\left(\frac{\partial}{\partial z} \right)_r = \left(\frac{\partial}{\partial z} \right)_f - \frac{\partial R_i}{\partial z} \left(\frac{\partial}{\partial r} \right), \quad (\text{A12})$$

where $\hat{r} \equiv (r/R_i)$. We apply (A12) to w , and substitute the result into (A9) to obtain

$$\frac{\partial v_r}{\partial r} + \frac{v_r}{r} = - \left[\left(\frac{\partial w}{\partial z} \right)_f - \frac{\partial R_i}{\partial z} \left(\frac{\partial w}{\partial r} \right) \right]. \quad (\text{A13})$$

Applying (A12) to v_r and using (A13) and (A9), we get

$$\begin{aligned} \left(\frac{\partial v_r}{\partial z} \right)_r &= \left(\frac{\partial v_r}{\partial z} \right)_f + \frac{\partial R_i}{\partial z} \left(\frac{\partial w}{\partial z} + \frac{v_r}{r} \right) \\ &= \left(\frac{\partial v_r}{\partial z} \right)_f + \frac{\partial R_i}{\partial z} \left[\left(\frac{\partial w}{\partial z} \right)_f - \frac{\partial R_i}{\partial z} \left(\frac{\partial w}{\partial r} \right) \right] \\ &\quad + \frac{\partial R_i}{\partial z} \frac{v_r}{r}. \end{aligned} \quad (\text{A14})$$

Substituting (A14) and (A12) applied to w in the brackets on the rhs of (A11), we obtain

$$\begin{aligned} r \frac{\partial w}{\partial r} \frac{\partial v_r}{\partial z} + r \left(\frac{\partial w}{\partial z} \right)^2 + v_r \left(\frac{\partial w}{\partial z} + \frac{v_r}{r} \right) &= \\ r \frac{\partial w}{\partial r} \left[\left(\frac{\partial v_r}{\partial z} \right)_f - \left(\frac{\partial w}{\partial z} \right)_f \frac{\partial R_i}{\partial z} \right] + r \left(\frac{\partial w}{\partial z} \right)_f^2 + v_r \left(\frac{\partial w}{\partial z} \right)_f + \frac{v_r^2}{r}. \end{aligned} \quad (\text{A15})$$

We substitute (A15) and (A12) applied to θ into (A11) to obtain

$$\begin{aligned} & \frac{\partial}{\partial r} \left[r \frac{\partial}{\partial r} \left(\frac{p'}{\rho} \right) \right] + r \frac{\partial^2}{\partial z^2} \left(\frac{p'}{\rho} \right) = \\ & -2 \left\{ r \frac{\partial w}{\partial r} \left[\left(\frac{\partial v_r}{\partial z} \right)_f - \left(\frac{\partial w}{\partial z} \right)_f \frac{\partial R_i}{\partial z} \right] + r \left(\frac{\partial w}{\partial z} \right)_f^2 \right. \\ & \left. + v_r \left(\frac{\partial w}{\partial z} \right)_f + \frac{v_r^2}{r} \right\} + r \frac{g}{\theta_0} \left[\left(\frac{\partial \theta'_v}{\partial z} \right)_f - \frac{\partial R_i}{\partial z} \left(\frac{\partial \theta'_v}{\partial z} \right) \right]. \end{aligned} \tag{A16}$$

Equation (A16) is equivalent to (A11) with one important exception. The only quantities on the rhs of (A16) that go to infinity across the updraft–downdraft boundary are $(\partial w/\partial r)$ and $(\partial \theta'_v/\partial r)$. Everything else remains finite. Thus, we can radially integrate this across the updraft–downdraft boundary.

The only term left to address with the coordinate

transformation is the $(\partial^2/\partial z^2)(p'/\rho)$ term of (A16). We apply (A12) to this term to get

$$\begin{aligned} \left[\frac{\partial^2}{\partial z^2} \left(\frac{p'}{\rho} \right) \right]_r &= \left\{ \frac{\partial \left[\frac{\partial}{\partial z} \left(\frac{p'}{\rho} \right) \right]}{\partial z} \right\}_f - \frac{\partial R_i}{\partial z} \frac{\partial}{\partial r} \left[\frac{\partial}{\partial z} \left(\frac{p'}{\rho} \right) \right]_r \\ &= \left[\frac{\partial^2}{\partial z^2} \left(\frac{p'}{\rho} \right) \right]_f - \frac{\partial^2 R_i}{\partial z^2} \frac{\partial}{\partial r} \left(\frac{p'}{\rho} \right) \\ &\quad - 2 \frac{\partial R_i}{\partial z} \frac{\partial}{\partial r} \left[\frac{\partial}{\partial z} \left(\frac{p'}{\rho} \right) \right]_f + \left(\frac{\partial R_i}{\partial z} \right)^2 \frac{\partial^2}{\partial r^2} \left(\frac{p'}{\rho} \right). \end{aligned} \tag{A17}$$

Using $(\partial/\partial r)[r(\partial/\partial r)(p'/\rho)] = r(\partial^2/\partial r^2)(p'/\rho) + (\partial/\partial r)(p'/\rho)$, we can write (A17) as

$$\begin{aligned} r \left[\frac{\partial^2}{\partial z^2} \left(\frac{p'}{\rho} \right) \right]_r &= r \left\{ \left[\frac{\partial^2}{\partial z^2} \left(\frac{p'}{\rho} \right) \right]_f - \frac{\partial^2 R_i}{\partial z^2} \frac{\partial}{\partial r} \left(\frac{p'}{\rho} \right) - 2 \frac{\partial R_i}{\partial z} \frac{\partial}{\partial r} \left[\frac{\partial}{\partial z} \left(\frac{p'}{\rho} \right) \right]_f \right. \\ &\quad \left. + \left(\frac{\partial R_i}{\partial z} \right)^2 \left\{ \frac{\partial}{\partial r} \left[r \frac{\partial}{\partial r} \left(\frac{p'}{\rho} \right) \right] + \frac{\partial}{\partial r} \left(\frac{p'}{\rho} \right) \right\} \right\} \\ &= r \left[\frac{\partial^2}{\partial z^2} \left(\frac{p'}{\rho} \right) \right]_f + \left[\left(\frac{\partial R_i}{\partial z} \right)^2 - r \frac{\partial^2 R_i}{\partial z^2} - 2 \frac{\partial R_i}{\partial z} \left(\frac{\partial}{\partial z} \right)_f \right] \frac{\partial}{\partial r} \left(\frac{p'}{\rho} \right) + \left(\frac{\partial R_i}{\partial z} \right)^2 \frac{\partial}{\partial r} \left[r \frac{\partial}{\partial r} \left(\frac{p'}{\rho} \right) \right]. \end{aligned} \tag{A18}$$

Substitute this into (A16) and rearrange to get

$$\begin{aligned} \left[1 + \left(\frac{\partial R_i}{\partial z} \right)^2 \right] \frac{\partial}{\partial r} \left[r \frac{\partial}{\partial r} \left(\frac{p'}{\rho} \right) \right] &= -2 \left\{ r \frac{\partial w}{\partial r} \left[\left(\frac{\partial v_r}{\partial z} \right)_f - \left(\frac{\partial w}{\partial z} \right)_f \frac{\partial R_i}{\partial z} \right] + r \left(\frac{\partial w}{\partial z} \right)_f^2 + v_r \left(\frac{\partial w}{\partial z} \right)_f + \frac{v_r^2}{r} \right\} \\ &\quad + r \frac{g}{\theta_0} \left[\left(\frac{\partial \theta'_v}{\partial z} \right)_f - \frac{\partial R_i}{\partial z} \left(\frac{\partial \theta'_v}{\partial z} \right) \right] - \left\{ r \left[\frac{\partial^2}{\partial z^2} \left(\frac{p'}{\rho} \right) \right]_f \right. \\ &\quad \left. + \left[\left(\frac{\partial R_i}{\partial z} \right)^2 - r \frac{\partial^2 R_i}{\partial z^2} - 2 \frac{\partial R_i}{\partial z} \left(\frac{\partial}{\partial z} \right)_f \right] \frac{\partial}{\partial r} \left(\frac{p'}{\rho} \right) \right\}. \end{aligned} \tag{A19}$$

We can now integrate (A19) across the boundary. The only terms that make a finite contribution to the integral are the ones that involve $(\partial w/\partial r)$ and $(\partial \theta'_v/\partial r)$. The $(\partial/\partial r)(p'/\rho)$ terms do not contribute because (p'/ρ) is continuous across the boundary. We find that

$$\begin{aligned} \left[1 + \left(\frac{\partial R_i}{\partial z} \right)^2 \right] R_i \left\{ \left[\frac{\partial}{\partial r} \left(\frac{p'}{\rho} \right) \right]_{R_i+\varepsilon} - \left[\frac{\partial}{\partial r} \left(\frac{p'}{\rho} \right) \right]_{R_i-\varepsilon} \right\} &= -2 \int_{R_i-\varepsilon}^{R_i+\varepsilon} r \frac{\partial w}{\partial r} \left[\left(\frac{\partial v_r}{\partial z} \right)_f - \left(\frac{\partial w}{\partial z} \right)_f \frac{\partial R_i}{\partial z} \right] dr \\ &\quad - R_i \frac{\partial R_i}{\partial z} \frac{g}{\theta_0} [(\theta'_{v,d}) - (\theta'_{v,u})]. \end{aligned} \tag{A20}$$

The integrand is a delta function times a step function. Unlike the delta function squared in Eq. (A11), this can be integrated. The result is

$$\left[1 + \left(\frac{\partial R_i}{\partial z}\right)^2\right] R_i \left\{ \left[\frac{\partial}{\partial r} \left(\frac{p'}{\rho} \right) \right]_{R_i+\varepsilon} - \left[\frac{\partial}{\partial r} \left(\frac{p'}{\rho} \right) \right]_{R_i-\varepsilon} \right\} = -R_i (w_d - w_u) \left\{ \left[\left(\frac{\partial v_r}{\partial z} \right)_{\hat{r}} \right]_{R_i+\varepsilon} + \left[\left(\frac{\partial v_r}{\partial z} \right)_{\hat{r}} \right]_{R_i-\varepsilon} \right. \\ \left. - \frac{\partial R_i}{\partial z} \left(\frac{\partial w_d}{\partial z} + \frac{\partial w_u}{\partial z} \right) \right\} - R_i \frac{\partial R_i}{\partial z} \frac{g}{\theta_0} [(\theta'_v)_d - (\theta'_v)_u] \quad (\text{A21})$$

or

$$\left\{ \left[\frac{\partial}{\partial r} \left(\frac{p'}{\rho} \right) \right]_{R_i+\varepsilon} - \left[\frac{\partial}{\partial r} \left(\frac{p'}{\rho} \right) \right]_{R_i-\varepsilon} \right\} = - \left[\frac{w_d - w_u}{1 + \left(\frac{\partial R_i}{\partial z}\right)^2} \right] \left\{ \left[\left(\frac{\partial v_r}{\partial z} \right)_{\hat{r}} \right]_{R_i+\varepsilon} + \left[\left(\frac{\partial v_r}{\partial z} \right)_{\hat{r}} \right]_{R_i-\varepsilon} \right\} \\ - \frac{\partial R_i}{\partial z} \left\{ \frac{(w_d - w_u) \left(\frac{\partial w_o}{\partial z} + \frac{\partial w_i}{\partial z} \right) + \frac{g}{\theta_0} [(\theta'_v)_d - (\theta'_v)_u]}{1 + \left(\frac{\partial R_i}{\partial z}\right)^2} \right\}. \quad (\text{A22})$$

Equation (A22) describes the jump in the pressure gradient across the updraft–downdraft boundary. All quantities are known from ADHOC2 (see LR05)

c. Outer cylinder

Combining (A6) and (A22), we obtain

$$\left[\frac{\partial}{\partial r} \left(\frac{p'}{\rho} \right) \right]_{R_i+\varepsilon} = \frac{R_i}{2} \left[B_u - \frac{3}{2} \left(\frac{\partial w_u}{\partial z} \right)^2 \right] - \frac{1}{R_i} \int_0^{R_i-\varepsilon} \left[r \frac{\partial^2}{\partial z^2} \left(\frac{p'}{\rho} \right) \right] dr - \left[\frac{w_d - w_u}{1 + \left(\frac{\partial R_i}{\partial z}\right)^2} \right] \left\{ \left[\left(\frac{\partial v_r}{\partial z} \right)_{\hat{r}} \right]_{R_i+\varepsilon} \right. \\ \left. + \left[\left(\frac{\partial v_r}{\partial z} \right)_{\hat{r}} \right]_{R_i-\varepsilon} \right\} - \frac{\partial R_i}{\partial z} \left\{ \frac{(w_d - w_u) \left(\frac{\partial w_d}{\partial z} + \frac{\partial w_u}{\partial z} \right) + \frac{g}{\theta_0} [(\theta'_v)_d - (\theta'_v)_u]}{1 + \left(\frac{\partial R_i}{\partial z}\right)^2} \right\}. \quad (\text{A23})$$

This is essentially an inner boundary condition for the outer region.

Using Eq. (6) and its radial derivative, the pressure Eq. (A1) for the outer cylinder is

$$\frac{1}{r} \frac{\partial}{\partial r} \left[r \frac{\partial}{\partial r} \left(\frac{p'}{\rho} \right) \right] + \frac{\partial^2}{\partial z^2} \left(\frac{p'}{\rho} \right) = -\frac{1}{2} \left(\frac{R_o^4}{r^4} + 3 \right) \left(\frac{\partial w_d}{\partial z} \right)^2 + B_d. \quad (\text{A24})$$

Outward integration of (A24) from $r = R_i + \varepsilon$ to $r = r$ gives

$$\frac{\partial}{\partial r} \left(\frac{p'}{\rho} \right) = \frac{R_i}{r} \left[\frac{\partial}{\partial r} \left(\frac{p'}{\rho} \right) \right]_{R_i+\varepsilon} + \frac{1}{4r} \left[\left(\frac{R_o^4}{r^2} - \frac{R_o^4}{R_i^2} \right) - 3(r^2 - R_i^2) \right] \left(\frac{\partial w_d}{\partial z} \right)^2 + \frac{B_d}{2r} (r^2 - R_i^2) \\ - \frac{1}{r} \int_{R_i+\varepsilon}^r \left[r \frac{\partial^2}{\partial z^2} \left(\frac{p'}{\rho} \right) \right] dr \quad \text{for } R_i < r \leq R_o. \quad (\text{A25})$$

Integrating a second time, we find that

$$\begin{aligned} \frac{p'(r)}{\rho} &= \frac{p'(R_i + \varepsilon)}{\rho} + \left\{ R_i \left[\frac{\partial}{\partial r} \left(\frac{p'}{\rho} \right) \right]_{R_i + \varepsilon} + \frac{1}{4} \left(-\frac{R_o^4}{R_i^2} + 3R_i^2 \right) \left(\frac{\partial w_d}{\partial z} \right)^2 - \frac{B_d}{2} R_i^2 \right\} \ln \left(\frac{r}{R_i} \right) \\ &\quad - \frac{1}{8} \left(\frac{\partial w_d}{\partial z} \right)^2 \left[R_o^4 \left(\frac{1}{r^2} - \frac{1}{R_i^2} \right) + 3(r^2 - R_i^2) \right] + \frac{(r^2 - R_i^2)}{4} B_d - \int_{R_i + \varepsilon}^r \left\{ \frac{1}{r} \int_{R_i + \varepsilon}^r \left[r \frac{\partial^2}{\partial z^2} \left(\frac{p'}{\rho} \right) \right] dr \right\} dr \end{aligned} \tag{A26}$$

for $R_i < r \leq R_o$.

We apply Leibniz’s rule to the last term in (A26) in order to pull the z derivatives out of the integral [see explanation for Eq. (A8) where we did the same]. This gives

$$\begin{aligned} \frac{p'(r)}{\rho} &= \frac{p'(R_i + \varepsilon)}{\rho} + \left\{ R_i \left[\frac{\partial}{\partial r} \left(\frac{p'}{\rho} \right) \right]_{R_i + \varepsilon} + \frac{1}{4} \left(-\frac{R_o^4}{R_i^2} + 3R_i^2 \right) \left(\frac{\partial w_d}{\partial z} \right)^2 - \frac{B_d}{2} R_i^2 \right\} \ln \left(\frac{r}{R_i} \right) \\ &\quad - \frac{1}{8} \left(\frac{\partial w_d}{\partial z} \right)^2 \left[R_o^4 \left(\frac{1}{r^2} - \frac{1}{R_i^2} \right) + 3(r^2 - R_i^2) \right] + \frac{(r^2 - R_i^2)}{4} B_d - \frac{\partial^2}{\partial z^2} \left\{ \int_{(R_i + \varepsilon)}^r \frac{1}{r} \left[\int_{(R_i + \varepsilon)}^r (rp) dr \right] dr \right\} \\ &\quad + \left[R_i p(R_i) \frac{\partial^2 R_i}{\partial z^2} + 2 \frac{\partial}{\partial z} [R_i p(R_i)] \frac{\partial R_i}{\partial z} \right] \ln \frac{r}{R_i} \text{ for } R_i < r \leq R_o. \end{aligned} \tag{A27}$$

There is no contribution to p at $r = R_i$ because $(\partial p / \partial r)$ is a step function there. Now, we use boundary condition (16) in Eq. (A8) and plug the result into (A27) to obtain

$$\begin{aligned} \frac{p'(r)}{\rho} &= \frac{p'(0)}{\rho} + \left\{ R_i \left[\frac{\partial}{\partial r} \left(\frac{p'}{\rho} \right) \right]_{R_i + \varepsilon} + \frac{1}{4} \left(-\frac{R_o^4}{R_i^2} + 3R_i^2 \right) \left(\frac{\partial w_d}{\partial z} \right)^2 - \frac{B_d}{2} R_i^2 \right\} \ln \left(\frac{r}{R_i} \right) \\ &\quad - \frac{1}{8} \left(\frac{\partial w_d}{\partial z} \right)^2 \left[R_o^4 \left(\frac{1}{r^2} - \frac{1}{R_i^2} \right) + 3(r^2 - R_i^2) \right] + \frac{(r^2 - R_i^2)}{4} B_d - \frac{\partial^2}{\partial z^2} \left\{ \int_{(R_i + \varepsilon)}^r \frac{1}{r} \left[\int_{(R_i + \varepsilon)}^r (rp) dr \right] dr \right\} \\ &\quad + \left[R_i p(R_i) \frac{\partial^2 R_i}{\partial z^2} + 2 \frac{\partial}{\partial z} [R_i p(R_i)] \frac{\partial R_i}{\partial z} \right] \ln \frac{r}{R_i} + B_u \left(\frac{R_i^2}{4} \right) - \frac{3R_i^2}{8} \left(\frac{\partial w_u}{\partial z} \right)^2 - \frac{\partial^2}{\partial z^2} \left\{ \int_0^{(R_i - \varepsilon)} \frac{1}{r} \left[\int_0^r (rp) dr \right] dr \right\} \\ &\quad - \left(\frac{\partial^2 R_i}{\partial z^2} \right) \left[\frac{1}{R_i} \int_0^{(R_i - \varepsilon)} (rp) dr \right] - 2 \left(\frac{\partial R_i}{\partial z} \right) \frac{\partial}{\partial z} \left[\frac{1}{R_i} \int_0^{(R_i - \varepsilon)} (rp) dr \right] \text{ for } R_i < r \leq R_o. \end{aligned} \tag{A28}$$

The total solution for the pressure field is given by Eqs. (A5) and (A28). The only thing left to do is to ensure that the boundary condition given by (15) holds true in Eq. (A28).

To enforce this condition, we can apply (A25) at $r = R_o$ and use boundary condition (15) to get

$$0 = R_i \left[\frac{\partial}{\partial r} \left(\frac{p'}{\rho} \right) \right]_{R_i + \varepsilon} + \frac{1}{4} \left[R_o^2 \left(1 - \frac{R_o^2}{R_i^2} \right) - 3(R_o^2 - R_i^2) \right] \left(\frac{\partial w_d}{\partial z} \right)^2 + \frac{B_d}{2} (R_o^2 - R_i^2) - \int_{R_i + \varepsilon}^{R_o} \left[r \frac{\partial^2}{\partial z^2} \left(\frac{p'}{\rho} \right) \right] dr. \tag{A29}$$

Substituting from (A23), we can rewrite (A29) as

$$\begin{aligned}
\int_0^{R_i-\varepsilon} \left[r \frac{\partial^2}{\partial z^2} \left(\frac{p'}{\rho} \right) \right] dr + \int_{R_i+\varepsilon}^{R_o} \left[r \frac{\partial^2}{\partial z^2} \left(\frac{p'}{\rho} \right) \right] dr = & \left[B_i \left(\frac{R_i^2}{2} \right) + \frac{B_o}{2} (R_o^2 - R_i^2) \right] \\
& - \frac{3R_i^2}{4} \left(\frac{\partial w_i}{\partial z} \right)^2 + \frac{1}{4} \left[R_o^2 \left(1 - \frac{R_o^2}{R_i^2} \right) - 3(R_o^2 - R_i^2) \right] \left(\frac{\partial w_o}{\partial z} \right)^2 \\
& - R_i \left[\frac{w_o - w_i}{1 + \left(\frac{\partial R_i}{\partial z} \right)^2} \right] \left\{ \left[\left(\frac{\partial v_r}{\partial z} \right) \right]_{r=R_i+\varepsilon} + \left[\left(\frac{\partial v_r}{\partial z} \right) \right]_{r=R_i-\varepsilon} \right\} \\
& - R_i \frac{\partial R_i}{\partial z} \left\{ \frac{(w_o - w_i) \left(\frac{\partial w_o}{\partial z} + \frac{\partial w_i}{\partial z} \right) + \frac{g}{\theta_0} [(\theta'_v)_o - (\theta'_v)_i]}{1 + \left(\frac{\partial R_i}{\partial z} \right)^2} \right\}.
\end{aligned} \tag{A30}$$

Enforcing (A30) is a way to insure that the boundary condition given by (15) is true. We cannot enforce (A30) by choosing the value of R_o , because R_o would then vary with height, and that would conflict with our assumption that R_o is independent of height. We cannot enforce (A30) by choosing the value of R_i , because R_i is already determined by the cloud model. It appears that the only way to enforce (A30) is by using it to determine the quantity on its lhs; that is,

$$\int_0^{R_i-\varepsilon} \left[r \frac{\partial^2}{\partial z^2} \left(\frac{p'}{\rho} \right) \right] dr + \int_{R_i+\varepsilon}^{R_o} \left[r \frac{\partial^2}{\partial z^2} \left(\frac{p'}{\rho} \right) \right] dr.$$

APPENDIX B

Derivation of Pressure Parameterization for the $\overline{u'u'}$ and $\overline{w'w'}$ Equations for the Clear Convective Case

The expressions needed for the $\overline{u'u'}$ and $\overline{w'w'}$ equations are

$$\frac{\partial}{\partial t} \overline{u'u'} \sim -2 \frac{\overline{u'}}{\rho} \frac{\partial \overline{p}}{\partial x} \quad \text{and} \quad \frac{\partial}{\partial t} \overline{w'w'} \sim -2 \frac{\overline{w'}}{\rho} \frac{\partial \overline{p}}{\partial z}. \tag{B1}$$

We can express the rhs of (B3) using

$$\frac{\overline{u'}}{\rho} \frac{\partial \overline{p}}{\partial x} = \frac{\overline{U'}}{\rho} \frac{\partial \overline{p}}{\partial r} \cos^2 \phi = \frac{1}{\pi R_o^2} \left(\int_0^{R_i} \int_0^{2\pi} \frac{U'}{\rho} \frac{\partial p}{\partial r} + \int_{R_i}^{R_o} \int_0^{2\pi} \frac{U'}{\rho} \frac{\partial p}{\partial r} \right) \cos^2 \phi \, d\phi \, dr. \tag{B7}$$

For the plume case, we can write

$$\frac{\overline{\partial p}}{\partial x} = \frac{\overline{\partial p}}{\partial r} \cos \phi \quad \text{and} \quad U' = u' \cos \phi, \tag{B2}$$

where ϕ is the angle between the radial vector and the x axis and U' is the total perturbation wind vector. This allows us to write (B1) as

$$\frac{\partial}{\partial t} \overline{u'u'} \sim -2 \frac{\overline{U'}}{\rho} \frac{\partial \overline{p}}{\partial r} \cos^2 \phi. \tag{B3}$$

We know $\partial p'/\partial r$ for the updraft and downdraft from Eqs. (A3) and (A25), respectively. We can derive an expression for U' if we use the continuity equation for axisymmetric motion (see LR05),

$$\frac{1}{r} \frac{\partial}{\partial r} (rU') = - \frac{\partial}{\partial z} w'. \tag{B4}$$

Integrating (B4) in r , we get

$$U' = - \frac{r}{2} \frac{\partial w_u}{\partial z} \quad \text{for} \quad r \leq R_i \tag{B5}$$

and

$$U' = \frac{1}{2r} (R_o^2 - r^2) \left(\frac{\partial w_d}{\partial z} \right) \quad \text{for} \quad R_i < r \leq R_o. \tag{B6}$$

Using (A3), (A25), (B5), and (B6), in (B7) and integrating in ϕ and r , we get

$$\begin{aligned} \frac{\overline{u' \partial p}}{\rho \partial x} = & \frac{1}{R_o^2} \left\{ \frac{-R_i^4}{16} \left(\frac{\partial w_u}{\partial z} \right) \left[B_u - \frac{3}{2} \left(\frac{\partial w_u}{\partial z} \right)^2 \right] + \frac{R_i}{2\rho} \left(\frac{\partial w_d}{\partial z} \right) \left(\frac{\partial p}{\partial r} \right)_{R_i+\varepsilon} \left(R_o^2 \ln \frac{R_o}{R_i} - \frac{R_o^2 - R_i^2}{2} \right) \right\} \\ & + \frac{1}{8R_o^2} \left(\frac{\partial w_d}{\partial z} \right)^3 \left[\left(\frac{R_o^6}{R_i^2} - \frac{7R_o^4}{4} + \frac{3R_i^4}{4} \right)^3 - \left(\frac{R_o^6}{R_i^2} - 3R_o^2 R_i^2 + R_o^4 \right) \ln \frac{R_o}{R_i} \right] + \frac{B_d}{16R_o^2} \left(\frac{\partial w_d}{\partial z} \right) [R_o^4 - R_i^4] \\ & - \frac{1}{R_o^2} \left\{ \int_0^{R_i} \frac{r}{2} \left(\frac{\partial w_u}{\partial z} \right) \left[\int_0^r r \frac{\partial^2}{\partial z^2} \left(\frac{p}{\rho} \right) dr \right] dr \right\} + \frac{1}{R_o^2} \left\{ \int_{R_i}^{R_o} \frac{(r^2 - R_o^2)}{2} \left(\frac{\partial w_d}{\partial z} \right) \left[\int_{(R_i+\varepsilon)}^r r \frac{\partial^2}{\partial z^2} \left(\frac{p}{\rho} \right) dr \right] dr \right\}. \end{aligned} \tag{B8}$$

APPENDIX C

Horizontal Solution for the Pressure in the Roll Case

a. The updraft and downdraft

We begin by radially integrating Eq. (40) over the updraft region, using the expression given by (36) for $u(x)$. We also use the mass-flux assumption that the vertical velocity and potential temperature are horizontally uniform within the updraft. We can then write (40) for the updraft as

$$\begin{aligned} \frac{\partial^2}{\partial x^2} \left(\frac{p'}{\rho} \right) = & -2 \left(\frac{\partial w_u}{\partial z} \right)^2 + B_u - \frac{\partial^2}{\partial z^2} \left(\frac{p'}{\rho} \right) \\ \text{for } & x_0 < x < x_1. \end{aligned} \tag{C1}$$

Integration of (C1) from $x = x_0 + \varepsilon$ to $x = x$ gives

$$\begin{aligned} \frac{\partial}{\partial x} \left(\frac{p'}{\rho} \right) = & \left[\frac{\partial}{\partial x} \left(\frac{p'}{\rho} \right) \right]_{x_0+\varepsilon} \\ & + (x - x_0) \left[-2 \left(\frac{\partial w_u}{\partial z} \right)^2 + B_u \right] \\ & - \int_{x_0+\varepsilon}^x \frac{\partial^2}{\partial z^2} \left(\frac{p'}{\rho} \right) dx \text{ for } x_0 < x < x_1. \end{aligned} \tag{C2}$$

Here we allow the possibility that $(\partial/\partial x)(p'/\rho)$ is discontinuous at the updraft–downdraft boundary. Integrating a second time gives

$$\begin{aligned} \frac{p'}{\rho} = & \left(\frac{p'}{\rho} \right)_{x_0} + (x - x_0) \left[\frac{\partial}{\partial x} \left(\frac{p'}{\rho} \right) \right]_{x_0+\varepsilon} + \frac{(x - x_0)^2}{2} \\ & \times \left[-2 \left(\frac{\partial w_u}{\partial z} \right)^2 + B_u \right] \\ & - \int_{x_0+\varepsilon}^x \left[\int_{x_0+\varepsilon}^x \frac{\partial^2}{\partial z^2} \left(\frac{p'}{\rho} \right) dx \right] dx \text{ for } x_0 < x < x_1. \end{aligned} \tag{C3}$$

In (C3), we have written $(p'/\rho)_{x_0}$ rather than $(p'/\rho)_{x_0+\varepsilon}$, since the pressure must be continuous.

For the downdraft, corresponding to (C2), we have

$$\begin{aligned} \frac{\partial}{\partial x} \left(\frac{p'}{\rho} \right) = & \left[\frac{\partial}{\partial x} \left(\frac{p'}{\rho} \right) \right]_{x_1+\varepsilon} + (x - x_1) \\ & \times \left[-2 \left(\frac{\partial w_d}{\partial z} \right)^2 + B_d \right] - \int_{x_1+\varepsilon}^x \frac{\partial^2}{\partial z^2} \left(\frac{p'}{\rho} \right) dx \\ \text{for } & x_1 < x < x_2, \end{aligned} \tag{C4}$$

and corresponding to (C3)

$$\begin{aligned} \frac{p'}{\rho} = & \left(\frac{p'}{\rho} \right)_{x_1} + (x - x_1) \left[\frac{\partial}{\partial x} \left(\frac{p'}{\rho} \right) \right]_{x_1+\varepsilon} + \frac{(x - x_1)^2}{2} \\ & \times \left[-2 \left(\frac{\partial w_d}{\partial z} \right)^2 + B_d \right] - \int_{x_1+\varepsilon}^x \left[\int_{x_1+\varepsilon}^x \frac{\partial^2}{\partial z^2} \left(\frac{p'}{\rho} \right) dx \right] dx \\ \text{for } & x_1 < x < x_2. \end{aligned} \tag{C5}$$

A special case of (C2) is

$$\begin{aligned} \left[\frac{\partial}{\partial x} \left(\frac{p'}{\rho} \right) \right]_{x_1-\varepsilon} &= \left[\frac{\partial}{\partial x} \left(\frac{p'}{\rho} \right) \right]_{x_0+\varepsilon} \\ &+ L_u \left[-2 \left(\frac{\partial w_u}{\partial z} \right)^2 + B_u \right] \\ &- \int_{x_0+\varepsilon}^{x_1-\varepsilon} \frac{\partial^2}{\partial z^2} \left(\frac{p'}{\rho} \right) dx, \end{aligned} \tag{C6}$$

where L_u is defined by (32). Similarly, a special case of (C3) is

$$\begin{aligned} \left(\frac{p'}{\rho} \right)_{x_1} &= \left(\frac{p'}{\rho} \right)_{x_0} + L_u \left[\frac{\partial}{\partial x} \left(\frac{p'}{\rho} \right) \right]_{x_0+\varepsilon} \\ &+ \frac{L_u^2}{2} \left[-2 \left(\frac{\partial w_u}{\partial z} \right)^2 + B_u \right] \\ &- \int_{x_0+\varepsilon}^{x_1-\varepsilon} \left[\int_{x_0+\varepsilon}^x \frac{\partial^2}{\partial z^2} \left(\frac{p'}{\rho} \right) dx \right] dx. \end{aligned} \tag{C7}$$

A special case of (C4) is

$$\begin{aligned} \left[\frac{\partial}{\partial x} \left(\frac{p'}{\rho} \right) \right]_{x_0-\varepsilon} &= \\ &\left[\frac{\partial}{\partial x} \left(\frac{p'}{\rho} \right) \right]_{x_1+\varepsilon} + L_d \left[-2 \left(\frac{\partial w_d}{\partial z} \right)^2 + B_d \right] \\ &- \int_{x_1+\varepsilon}^{x_2-\varepsilon} \frac{\partial^2}{\partial z^2} \left(\frac{p'}{\rho} \right) dx. \end{aligned} \tag{C8}$$

Here we have used the periodicity of the rolls to replace $[(\partial/\partial x)(p'/\rho)]_{x_2-\varepsilon}$ by $[(\partial/\partial x)(p'/\rho)]_{x_0-\varepsilon}$. Finally, a special case of (C5) is

$$\begin{aligned} \left(\frac{p'}{\rho} \right)_{x_0} &= \left(\frac{p'}{\rho} \right)_{x_1} + L_d \left[\frac{\partial}{\partial x} \left(\frac{p'}{\rho} \right) \right]_{x_1+\varepsilon} \\ &+ \frac{L_d^2}{2} \left[-2 \left(\frac{\partial w_d}{\partial z} \right)^2 + B_d \right] \\ &- \int_{x_1+\varepsilon}^{x_2-\varepsilon} \left[\int_{x_1+\varepsilon}^x \frac{\partial^2}{\partial z^2} \left(\frac{p'}{\rho} \right) dx \right] dx. \end{aligned} \tag{C9}$$

Adding (C7) and (C9), we find that

$$\begin{aligned} 2 \left\{ L_u \left[\frac{\partial}{\partial x} \left(\frac{p'}{\rho} \right) \right]_{x_0+\varepsilon} + L_d \left[\frac{\partial}{\partial x} \left(\frac{p'}{\rho} \right) \right]_{x_1+\varepsilon} \right\} &= \\ + 2 \left[\left(L_u \frac{\partial w_u}{\partial z} \right)^2 + \left(L_d \frac{\partial w_d}{\partial z} \right)^2 \right] - (L_u^2 B_u + L_d^2 B_d) & \\ + (C + D), & \end{aligned} \tag{C10}$$

where

$$\begin{aligned} C &\equiv 2 \int_{x_0+\varepsilon}^{x_1-\varepsilon} \left[\int_{x_0+\varepsilon}^x \frac{\partial^2}{\partial z^2} \left(\frac{p'}{\rho} \right) dx \right] dx \quad \text{and} \\ D &\equiv 2 \int_{x_1+\varepsilon}^{x_2-\varepsilon} \left[\int_{x_1+\varepsilon}^x \frac{\partial^2}{\partial z^2} \left(\frac{p'}{\rho} \right) dx \right] dx. \end{aligned} \tag{C11}$$

Equation (C10) will be used later.

Note that it is not possible to solve for either $(p'/\rho)_{x_0}$ or $(p'/\rho)_{x_1}$ without further information; only their difference is determined. To complete the solution, we assume that the domain average of the perturbation pressure is zero; that is,

$$\int_{x_0+\varepsilon}^{x_1-\varepsilon} p \, dx + \int_{x_1+\varepsilon}^{x_2-\varepsilon} p \, dx = 0. \tag{C12}$$

Substitute into (C12) from (C3) and (C5):

$$\begin{aligned} \left(\frac{p'}{\rho} \right)_{x_0} L_u + \frac{L_u^2}{2} \left[\frac{\partial}{\partial x} \left(\frac{p'}{\rho} \right) \right]_{x_0+\varepsilon} + \frac{L_u^3}{6} \left[-2 \left(\frac{\partial w_u}{\partial z} \right)^2 + B_u \right] &- \int_{x_0+\varepsilon}^{x_1-\varepsilon} \left\{ \int_{x_0+\varepsilon}^x \left[\int_{x_0+\varepsilon}^x \frac{\partial^2}{\partial z^2} \left(\frac{p'}{\rho} \right) dx \right] dx \right\} dx \\ + \left(\frac{p'}{\rho} \right)_{x_1} L_d + \frac{L_d^2}{2} \left[\frac{\partial}{\partial x} \left(\frac{p'}{\rho} \right) \right]_{x_1+\varepsilon} + \frac{L_d^3}{6} \left[-2 \left(\frac{\partial w_d}{\partial z} \right)^2 + B_d \right] &- \int_{x_1+\varepsilon}^{x_2-\varepsilon} \left\{ \int_{x_1+\varepsilon}^x \left[\int_{x_1+\varepsilon}^x \frac{\partial^2}{\partial z^2} \left(\frac{p'}{\rho} \right) dx \right] dx \right\} dx = 0. \end{aligned} \tag{C13}$$

Adding (C6) and (C8) gives

$$0 = \left\{ \left[\frac{\partial}{\partial x} \left(\frac{p'}{\rho} \right) \right]_{x_0+\varepsilon} - \left[\frac{\partial}{\partial x} \left(\frac{p'}{\rho} \right) \right]_{x_0-\varepsilon} \right\} + \left\{ \left[\frac{\partial}{\partial x} \left(\frac{p'}{\rho} \right) \right]_{x_1+\varepsilon} - \left[\frac{\partial}{\partial x} \left(\frac{p'}{\rho} \right) \right]_{x_1-\varepsilon} \right\} - 2 \left[L_u \left(\frac{\partial w_u}{\partial z} \right)^2 + L_d \left(\frac{\partial w_d}{\partial z} \right)^2 \right] + (L_u B_u + L_d B_d) - \left[\int_{x_0+\varepsilon}^{x_1-\varepsilon} \frac{\partial^2}{\partial z^2} \left(\frac{p'}{\rho} \right) dx + \int_{x_1+\varepsilon}^{x_2-\varepsilon} \frac{\partial^2}{\partial z^2} \left(\frac{p'}{\rho} \right) dx \right]. \tag{C14}$$

b. The updraft–downdraft boundary

The horizontal pressure gradient can be discontinuous at the updraft–downdraft boundary when the boundary is tilted. In addition, vertical derivatives can be infinite at the boundary when it is tilted. Thus, in order to integrate the pressure equation [Eq. (40)] across this boundary, we introduce the coordinate transformation

$$\left(\frac{\partial}{\partial z} \right)_x = \left(\frac{\partial}{\partial z} \right)_x - \frac{\partial x_1}{\partial z} \left(\frac{\partial}{\partial x} \right), \tag{C15}$$

where $\hat{x} \equiv x - x_1(z)$ is defined so that it is independent of height along the boundary. Using (C15) applied to u , w , and θ , and referring to (11) and (35), we can rewrite (40) as

$$\frac{\partial^2}{\partial x^2} \left(\frac{p'}{\rho} \right) + \left[\frac{\partial^2}{\partial z^2} \left(\frac{p'}{\rho} \right) \right]_x = -2 \left\{ \frac{\partial w}{\partial x} \left[\left(\frac{\partial u}{\partial z} \right)_{\hat{x}} - \left(\frac{\partial w}{\partial z} \right)_{\hat{x}} \frac{\partial x_1}{\partial z} \right] + \left(\frac{\partial w}{\partial z} \right)_{\hat{x}}^2 \right\} + \frac{g}{\theta_0} \left[\left(\frac{\partial \theta'_v}{\partial z} \right)_{\hat{x}} - \frac{\partial x_1}{\partial z} \left(\frac{\partial \theta'_v}{\partial x} \right) \right]. \tag{C16}$$

We also need to deal with the $[(\partial^2/\partial z^2)(p'/\rho)]_x$ term on the lhs of (C16). Using (C15) for this term and substituting the result into the lhs of (C16), we rearrange to obtain

$$\left[1 + \left(\frac{\partial x_1}{\partial z} \right)^2 \right] \frac{\partial^2}{\partial x^2} \left(\frac{p'}{\rho} \right) = -2 \left\{ \frac{\partial w}{\partial x} \left[\left(\frac{\partial u}{\partial z} \right)_{\hat{x}} - \left(\frac{\partial w}{\partial z} \right)_{\hat{x}} \frac{\partial x_1}{\partial z} \right] + \left(\frac{\partial w}{\partial z} \right)_{\hat{x}}^2 \right\} + \frac{g}{\theta_0} \left[\left(\frac{\partial \theta'_v}{\partial z} \right)_{\hat{x}} - \frac{\partial x_1}{\partial z} \left(\frac{\partial \theta'_v}{\partial x} \right) \right] - \left[\frac{\partial^2}{\partial z^2} \left(\frac{p'}{\rho} \right) \right]_{\hat{x}} + \frac{\partial^2 x_1}{\partial z^2} \left[\frac{\partial}{\partial x} \left(\frac{p'}{\rho} \right) \right] + 2 \frac{\partial x_1}{\partial z} \frac{\partial}{\partial x} \left[\left[\frac{\partial}{\partial z} \left(\frac{p'}{\rho} \right) \right]_{\hat{x}} \right]. \tag{C17}$$

We can now do the integral across the boundary. The only terms that make finite contributions to the integral are the ones that involve $(\partial w/\partial x)$ and $(\partial \theta'_v/\partial x)$. The terms involving (p'/ρ) on the second line of the rhs of (C17) do not contribute because (p'/ρ) is continuous across the boundary. We obtain

$$\left[1 + \left(\frac{\partial x_1}{\partial z} \right)^2 \right] \left\{ \left[\frac{\partial}{\partial x} \left(\frac{p'}{\rho} \right) \right]_{x_1+\varepsilon} - \left[\frac{\partial}{\partial x} \left(\frac{p'}{\rho} \right) \right]_{x_1-\varepsilon} \right\} = -2 \int_{x_1-\varepsilon}^{x_1+\varepsilon} \frac{\partial w}{\partial x} \left[\left(\frac{\partial u}{\partial z} \right)_{\hat{x}} - \left(\frac{\partial w}{\partial z} \right)_{\hat{x}} \frac{\partial x_1}{\partial z} \right] dx - \frac{\partial x_1}{\partial z} \frac{g}{\theta_0} [(\theta'_v)_{x_1+\varepsilon} - (\theta'_v)_{x_1-\varepsilon}]. \tag{C18}$$

The integrand of the integral in (C18) now has the form of a delta function times a step function. Evaluating the integral and using $w_{x_1-\varepsilon} = w_u$, $w_{x_1+\varepsilon} = w_d$, $(\theta'_v)_{x_1-\varepsilon} = (\theta'_v)_u$, and $(\theta'_v)_{x_1+\varepsilon} = (\theta'_v)_d$, we find, after rearranging, that

$$\left[\frac{\partial}{\partial x} \left(\frac{p'}{\rho} \right) \right]_{x_1+\varepsilon} - \left[\frac{\partial}{\partial x} \left(\frac{p'}{\rho} \right) \right]_{x_1-\varepsilon} = \left[\frac{w_u - w_d}{1 + \left(\frac{\partial x_1}{\partial z} \right)^2} \right] \left\{ \left[\left(\frac{\partial u}{\partial z} \right)_{\hat{x}} \right]_{x_1+\varepsilon} + \left[\left(\frac{\partial u}{\partial z} \right)_{\hat{x}} \right]_{x_1-\varepsilon} \right\} + \frac{\partial x_1}{\partial z} \left\{ \frac{(w_u - w_d) \left(\frac{\partial w_u}{\partial z} + \frac{\partial w_d}{\partial z} \right) + \frac{g}{\theta_0} [(\theta'_v)_u - (\theta'_v)_d]}{1 + \left(\frac{\partial x_1}{\partial z} \right)^2} \right\}. \tag{C19}$$

The corresponding result for the x_0 boundary can be obtained by using a suitably altered definition of \hat{x} , and is very similar to (C19):

$$\left[\frac{\partial}{\partial x} \left(\frac{p'}{\rho} \right) \right]_{x_0+\varepsilon} - \left[\frac{\partial}{\partial x} \left(\frac{p'}{\rho} \right) \right]_{x_0-\varepsilon} = - \left[\frac{w_u - w_d}{1 + \left(\frac{\partial x_0}{\partial z} \right)^2} \right] \left\{ \left[\left(\frac{\partial u}{\partial z} \right)_{\hat{x}} \right]_{x_0+\varepsilon} + \left[\left(\frac{\partial u}{\partial z} \right)_{\hat{x}} \right]_{x_0-\varepsilon} \right\} - \frac{\partial x_0}{\partial z} \left\{ \frac{(w_u - w_d) \left(\frac{\partial w_u}{\partial z} + \frac{\partial w_d}{\partial z} \right) + \frac{g}{\theta_0} [(\theta'_v)_u - (\theta'_v)_d]}{1 + \left(\frac{\partial x_0}{\partial z} \right)^2} \right\}. \tag{C20}$$

We can now use (C19) and (C20) in (C14), to obtain

$$0 = (w_u - w_d) \left[\left\{ \frac{\left[\left(\frac{\partial u}{\partial z} \right)_{\hat{x}} \right]_{x_1+\varepsilon} + \left[\left(\frac{\partial u}{\partial z} \right)_{\hat{x}} \right]_{x_1-\varepsilon}}{1 + \left(\frac{\partial x_1}{\partial z} \right)^2} \right\} - \left\{ \frac{\left[\left(\frac{\partial u}{\partial z} \right)_{\hat{x}} \right]_{x_0+\varepsilon} + \left[\left(\frac{\partial u}{\partial z} \right)_{\hat{x}} \right]_{x_0-\varepsilon}}{1 + \left(\frac{\partial x_0}{\partial z} \right)^2} \right\} \right] + \left[\frac{\frac{\partial x_1}{\partial z}}{1 + \left(\frac{\partial x_1}{\partial z} \right)^2} - \frac{\frac{\partial x_0}{\partial z}}{1 + \left(\frac{\partial x_0}{\partial z} \right)^2} \right] \left\{ (w_u - w_d) \left(\frac{\partial w_u}{\partial z} + \frac{\partial w_d}{\partial z} \right) + \frac{g}{\theta_0} [(\theta'_v)_u - (\theta'_v)_d] \right\} + L_u \left[-2 \left(\frac{\partial w_u}{\partial z} \right)^2 + B_u \right] + L_d \left[-2 \left(\frac{\partial w_d}{\partial z} \right)^2 + B_d \right] - \left[\int_{x_0+\varepsilon}^{x_1-\varepsilon} \frac{\partial^2}{\partial z^2} \left(\frac{p'}{\rho} \right) dx + \int_{x_1+\varepsilon}^{x_2-\varepsilon} \frac{\partial^2}{\partial z^2} \left(\frac{p'}{\rho} \right) dx \right]. \tag{C21}$$

This can only be interpreted as a constraint on $\int_{x_0+\varepsilon}^{x_1-\varepsilon} (\partial^2/\partial z^2)(p'/\rho) dx + \int_{x_1+\varepsilon}^{x_2-\varepsilon} (\partial^2/\partial z^2)(p'/\rho) dx$. Substituting from (C6) into (C19) and from (C8) into (C20), we obtain, respectively,

$$\left[\frac{\partial}{\partial x} \left(\frac{p'}{\rho} \right) \right]_{x_1+\varepsilon} = \left[\frac{\partial}{\partial x} \left(\frac{p'}{\rho} \right) \right]_{x_0+\varepsilon} + L_u \left[-2 \left(\frac{\partial w_u}{\partial z} \right)^2 + B_u \right] - \int_{(x_0+\varepsilon)}^{(x_1-\varepsilon)} \frac{\partial^2}{\partial z^2} \left(\frac{p'}{\rho} \right) dx + \left[\frac{w_u - w_d}{1 + \left(\frac{\partial x_1}{\partial z} \right)^2} \right] \times \left\{ \left[\left(\frac{\partial u}{\partial z} \right)_{\hat{x}} \right]_{x_1+\varepsilon} + \left[\left(\frac{\partial u}{\partial z} \right)_{\hat{x}} \right]_{x_1-\varepsilon} \right\} + \frac{\partial x_1}{\partial z} \left\{ \frac{(w_u - w_d) \left(\frac{\partial w_u}{\partial z} + \frac{\partial w_d}{\partial z} \right) + \frac{g}{\theta_0} [(\theta'_v)_u - (\theta'_v)_d]}{1 + \left(\frac{\partial x_1}{\partial z} \right)^2} \right\}. \tag{C22}$$

$$\left[\frac{\partial}{\partial x} \left(\frac{p'}{\rho} \right) \right]_{x_0+\varepsilon} - \left[\frac{\partial}{\partial x} \left(\frac{p'}{\rho} \right) \right]_{x_1+\varepsilon} = - \left[\frac{w_u - w_d}{1 + \left(\frac{\partial x_0}{\partial z} \right)^2} \right] \left\{ \left[\left(\frac{\partial u}{\partial z} \right)_{\hat{x}} \right]_{x_0+\varepsilon} + \left[\left(\frac{\partial u}{\partial z} \right)_{\hat{x}} \right]_{x_0-\varepsilon} \right\} - \frac{\partial x_0}{\partial z} \left\{ \frac{(w_u - w_d) \left(\frac{\partial w_u}{\partial z} + \frac{\partial w_d}{\partial z} \right) + \frac{g}{\theta_0} [(\theta'_v)_u - (\theta'_v)_d]}{1 + \left(\frac{\partial x_0}{\partial z} \right)^2} \right\} - L_d \left[-2 \left(\frac{\partial w_d}{\partial z} \right)^2 + B_d \right] + \int_{x_1+\varepsilon}^{x_2-\varepsilon} \frac{\partial^2}{\partial z^2} \left(\frac{p'}{\rho} \right) dx. \tag{C23}$$

Subtracting (C23) from (C22) gives a nice symmetrical form:

$$\begin{aligned}
 2\left\{\left[\frac{\partial}{\partial x}\left(\frac{p'}{\rho}\right)\right]_{x_1+\varepsilon}-\left[\frac{\partial}{\partial x}\left(\frac{p'}{\rho}\right)\right]_{x_0+\varepsilon}\right\} &= (w_u-w_d)\left[\frac{\left\{\left[\left(\frac{\partial u}{\partial z}\right)_{\hat{x}}\right]_{x_1+\varepsilon}+\left[\left(\frac{\partial u}{\partial z}\right)_{\hat{x}}\right]_{x_1-\varepsilon}\right\}}{1+\left(\frac{\partial x_1}{\partial z}\right)^2}\right. \\
 &+ \left.\frac{\left\{\left[\left(\frac{\partial u}{\partial z}\right)_{\hat{x}}\right]_{x_0+\varepsilon}+\left[\left(\frac{\partial u}{\partial z}\right)_{\hat{x}}\right]_{x_0-\varepsilon}\right\}}{1+\left(\frac{\partial x_0}{\partial z}\right)^2}\right], \\
 &+ \left[\frac{\frac{\partial x_1}{\partial z}}{1+\left(\frac{\partial x_1}{\partial z}\right)^2}+\frac{\frac{\partial x_0}{\partial z}}{1+\left(\frac{\partial x_0}{\partial z}\right)^2}\right]\left\{(w_u-w_d)\left(\frac{\partial w_u}{\partial z}+\frac{\partial w_d}{\partial z}\right)\right. \\
 &+ \left.\frac{g}{\theta_0}\left[(\theta'_{w_u})-(\theta'_{w_d})\right]-2\left[-L_u\left(\frac{\partial w_u}{\partial z}\right)^2+L_d\left(\frac{\partial w_d}{\partial z}\right)^2\right]\right. \\
 &+ \left.(-L_u B_u+L_d B_d)+E-F,\right. \tag{C24}
 \end{aligned}$$

where

$$E \equiv \int_{x_0+\varepsilon}^{x_1-\varepsilon} \frac{\partial^2}{\partial z^2} \left(\frac{p'}{\rho}\right) dx \quad \text{and} \quad F \equiv \int_{x_1+\varepsilon}^{x_2-\varepsilon} \frac{\partial^2}{\partial z^2} \left(\frac{p'}{\rho}\right) dx. \tag{C25}$$

Equation (C24) can be combined with (C10) to solve for the two unknowns $[(\partial/\partial x)(p'/\rho)]_{x_1+\varepsilon}$ and $[(\partial/\partial x)(p'/\rho)]_{x_0+\varepsilon}$.

Multiply (C24) by L_u , add to (C10), and simplify to obtain

$$\begin{aligned}
 2\left[\frac{\partial}{\partial x}\left(\frac{p'}{\rho}\right)\right]_{x_1+\varepsilon} &= 2\frac{L_u^2}{L}\left[2\left(\frac{\partial w_u}{\partial z}\right)^2-B_u\right]-\frac{L_d(L_u-L_d)}{L}\left[2\left(\frac{\partial w_d}{\partial z}\right)^2-B_d\right]+\frac{1}{L}(C+D)+\frac{L_u}{L}(E-F) \\
 &+ \frac{L_u}{L}(w_u-w_d)\left[\frac{\left\{\left[\left(\frac{\partial u}{\partial z}\right)_{\hat{x}}\right]_{x_1+\varepsilon}+\left[\left(\frac{\partial u}{\partial z}\right)_{\hat{x}}\right]_{x_1-\varepsilon}\right\}}{1+\left(\frac{\partial x_1}{\partial z}\right)^2}\right. \\
 &+ \left.\frac{\left\{\left[\left(\frac{\partial u}{\partial z}\right)_{\hat{x}}\right]_{x_0+\varepsilon}+\left[\left(\frac{\partial u}{\partial z}\right)_{\hat{x}}\right]_{x_0-\varepsilon}\right\}}{1+\left(\frac{\partial x_0}{\partial z}\right)^2}\right] \\
 &+ \frac{L_u}{L}\left[\frac{\frac{\partial x_1}{\partial z}}{1+\left(\frac{\partial x_1}{\partial z}\right)^2}+\frac{\frac{\partial x_0}{\partial z}}{1+\left(\frac{\partial x_0}{\partial z}\right)^2}\right]\left\{(w_u-w_d)\left(\frac{\partial w_u}{\partial z}+\frac{\partial w_d}{\partial z}\right)+\frac{g}{\theta_0}\left[(\theta'_{w_u})-(\theta'_{w_d})\right]\right\}. \tag{C26}
 \end{aligned}$$

Similarly, multiply (C24) by L_d , subtract from (C10), and simplify to obtain

$$\begin{aligned}
 2\left[\frac{\partial}{\partial x}\left(\frac{p'}{\rho}\right)\right]_{x_0+\varepsilon} &= 2\frac{L_d^2}{L}\left[2\left(\frac{\partial w_d}{\partial z}\right)^2-B_d\right]+\frac{L_u(L_u-L_d)}{L}\left[2\left(\frac{\partial w_u}{\partial z}\right)^2-B_u\right]+\frac{1}{L}(C+D)-\frac{L_d}{L}(E-F) \\
 &- \frac{L_d}{L}(w_u-w_d)\left[\frac{\left\{\left[\left(\frac{\partial u}{\partial z}\right)_{\hat{x}}\right]_{x_1+\varepsilon}+\left[\left(\frac{\partial u}{\partial z}\right)_{\hat{x}}\right]_{x_1-\varepsilon}\right\}}{1+\left(\frac{\partial x_1}{\partial z}\right)^2}\right. \\
 &+ \left.\frac{\left\{\left[\left(\frac{\partial u}{\partial z}\right)_{\hat{x}}\right]_{x_0+\varepsilon}+\left[\left(\frac{\partial u}{\partial z}\right)_{\hat{x}}\right]_{x_0-\varepsilon}\right\}}{1+\left(\frac{\partial x_0}{\partial z}\right)^2}\right] \\
 &- \frac{L_d}{L}\left[\frac{\frac{\partial x_1}{\partial z}}{1+\left(\frac{\partial x_1}{\partial z}\right)^2}+\frac{\frac{\partial x_0}{\partial z}}{1+\left(\frac{\partial x_0}{\partial z}\right)^2}\right]\left\{(w_u-w_d)\left(\frac{\partial w_u}{\partial z}+\frac{\partial w_d}{\partial z}\right)+\frac{g}{\theta_0}\left[(\theta'_{w_u})-(\theta'_{w_d})\right]\right\}. \tag{C27}
 \end{aligned}$$

We can now substitute (C26) and (C27) into (C5) and (C3), respectively, to get

$$\begin{aligned}
 0 = & \int_{x_0+\varepsilon}^{x_1-\varepsilon} \left\{ \left(\frac{p'}{\rho} \right)_{x_0+\varepsilon} + (x-x_0) \left[\frac{\partial}{\partial x} \left(\frac{p'}{\rho} \right) \right]_{x_0+\varepsilon} + \frac{(x-x_0)^2}{2} \left[-2 \left(\frac{\partial w_u}{\partial z} \right)^2 + B_u \right] \right\} dx \\
 & - \int_{x_0+\varepsilon}^{x_1-\varepsilon} \left\{ \int_{x_0+\varepsilon}^x \left[\int_{x_0+\varepsilon}^x \frac{\partial^2}{\partial z^2} \left(\frac{p'}{\rho} \right) dx \right] dx \right\} dx \\
 & + \int_{x_1+\varepsilon}^{x_2-\varepsilon} \left\{ \left(\frac{p'}{\rho} \right)_{x_0+\varepsilon} + L_u \left[\frac{\partial}{\partial x} \left(\frac{p'}{\rho} \right) \right]_{x_0+\varepsilon} + \frac{L_u^2}{2} \left[-2 \left(\frac{\partial w_u}{\partial z} \right)^2 + B_u \right] \right\} dx \\
 & + \int_{x_1+\varepsilon}^{x_2-\varepsilon} \left\{ (x-x_1) \left[\frac{\partial}{\partial x} \left(\frac{p'}{\rho} \right) \right]_{x_1+\varepsilon} + \frac{(x-x_1)^2}{2} \left[-2 \left(\frac{\partial w_d}{\partial z} \right)^2 + B_d \right] \right\} dx \\
 & - \int_{x_1+\varepsilon}^{x_2-\varepsilon} \left\{ \int_{x_0+\varepsilon}^{x_1-\varepsilon} \left[\int_{x_0+\varepsilon}^x \frac{\partial^2}{\partial z^2} \left(\frac{p'}{\rho} \right) dx \right] dx + \int_{x_1+\varepsilon}^x \left[\int_{x_1+\varepsilon}^x \frac{\partial^2}{\partial z^2} \left(\frac{p'}{\rho} \right) dx \right] dx \right\} dx. \tag{C28}
 \end{aligned}$$

Evaluating the (single) integrals, we get

$$\begin{aligned}
 \left(1 + \frac{L_d}{L_u} \right) \left(\frac{p'}{\rho} \right)_{x_0+\varepsilon} = & - \left\{ \frac{L_u}{2} \left[\frac{\partial}{\partial x} \left(\frac{p'}{\rho} \right) \right]_{x_0+\varepsilon} + \frac{L_u^2}{6} \left[-2 \left(\frac{\partial w_u}{\partial z} \right)^2 + B_u \right] \right\} \\
 & + \frac{1}{L_u} \int_{(x_0+\varepsilon)}^{(x_1-\varepsilon)} \left\{ \int_{(x_0+\varepsilon)}^x \left[\int_{(x_0+\varepsilon)}^x \frac{\partial^2}{\partial z^2} \left(\frac{p'}{\rho} \right) dx \right] dx \right\} dx \\
 & - L_d \left\{ \left[\frac{\partial}{\partial x} \left(\frac{p'}{\rho} \right) \right]_{x_0+\varepsilon} + \frac{L_u}{2} \left[-2 \left(\frac{\partial w_u}{\partial z} \right)^2 + B_u \right] \right\} \\
 & - \frac{L_d^2}{L_u} \left\{ \frac{1}{2} \left[\frac{\partial}{\partial x} \left(\frac{p'}{\rho} \right) \right]_{x_1+\varepsilon} + \frac{L_d}{6} \left[-2 \left(\frac{\partial w_d}{\partial z} \right)^2 + B_d \right] \right\} \\
 & + \frac{1}{L_u} \int_{(x_1+\varepsilon)}^{(x_2-\varepsilon)} \left\{ \int_{(x_0+\varepsilon)}^{(x_1-\varepsilon)} \left[\int_{(x_0+\varepsilon)}^x \frac{\partial^2}{\partial z^2} \left(\frac{p'}{\rho} \right) dx \right] dx + \int_{(x_1+\varepsilon)}^x \left[\int_{(x_1+\varepsilon)}^x \frac{\partial^2}{\partial z^2} \left(\frac{p'}{\rho} \right) dx \right] dx \right\} dx. \tag{C29}
 \end{aligned}$$

Substituting (C26) and (C27) into (C29), this equation can be solved for the $(p'/\rho)_{x_0+\varepsilon}$, the only unknown left. We now have known expressions for $(p'/\rho)_{x_0+\varepsilon}$, $[(\partial/\partial x)(p'/\rho)]_{x_0+\varepsilon}$, and $[(\partial/\partial x)(p'/\rho)]_{x_1+\varepsilon}$, and thus, the total solution for the pressure as a function of x and z [given by Eqs. (41) and (42)] is known.

and $(\partial p/\partial r)_{R_i+\varepsilon}$. The solution for $p'(0)$ is given by Eq. (24) and contains the additional unknown $(p)_{R_i+\varepsilon}$. The solution for $(p)_{R_i+\varepsilon}$ term is given by Eq. (A8) if we use boundary condition (16). The solution for $(\partial p/\partial r)_{R_i+\varepsilon}$ is given by Eq. (A23).

To solve this complex set of equations, we do the following steps:

APPENDIX D

Implementation Method for the Axisymmetric Free Convective Case

The solution for the pressure is given by Eqs. (21) and (22). These equations contain the unknowns $p'(0)$

- 1) Neglect all terms that contain double integrals of p and double derivatives with respect to z . This includes the last term in Eq. (21), the last three lines of Eq. (22), the last two lines of Eq. (24), the last term on the first line of (A23), and the last three terms of Eq. (A8). Once these are set to zero, the equations

contain only known quantities and can be solved directly for the pressure, p .

- 2) Integrate the expression we get for the pressure and evaluate the integral terms that we initially neglected.
- 3) Evaluate the double derivative terms (that we neglected) using the finite difference methods discussed in section 2a.
- 4) Plug the values obtained from steps 2 and 3 back into Eqs. (21), (22), (24), (A8), and (A23), and resolve the equations.
- 5) Iterate by going back to step 2 until the solution converges.

REFERENCES

- André, J. C., G. DeMoor, P. Lacarrère, G. Therry, and R. DuVachat, 1978: Modeling the 24-hour evolution of the mean and turbulent structures of the planetary boundary layer. *J. Atmos. Sci.*, **35**, 1861–1883.
- Bougeault, P., and J. C. André, 1986: On the stability of the third-order turbulence closure for the modeling of the stratocumulus-topped boundary layer. *J. Atmos. Sci.*, **43**, 1574–1581.
- Cheng, Y., V. M. Canuto, and A. M. Howard, 2002: An improved model for the turbulent PBL. *J. Atmos. Sci.*, **59**, 1550–1565.
- Chou, S.-H., and M. P. Ferguson, 1991: Heat fluxes and roll circulations over the western gulf stream during an intense cold-air outbreak. *Bound.-Layer Meteor.*, **55**, 255–281.
- Deardorff, J. W., 1972: Numerical investigation of neutral and unstable planetary boundary layers. *J. Atmos. Sci.*, **29**, 91–115.
- , 1974: Three-dimensional numerical study of the height and mean structure of a heated planetary boundary layer. *Bound.-Layer Meteor.*, **7**, 81–106.
- Glendening, J. W., 1996: Lineal eddy features under strong shear conditions. *J. Atmos. Sci.*, **53**, 3430–3449.
- Hicks, B. B., 1978: An analysis of Wangara micrometeorology surface stress, sensible heat, evaporation, and dewfall. NOAA Tech. Memo. ERL ARL-104, Air Resources Laboratories, Silver Springs, MD, 36 pp.
- Khairoutdinov, M., and D. A. Randall, 2003: Cloud-resolving modeling of ARM summer 1997 IOP: Model formulation, results, uncertainties, and sensitivities. *J. Atmos. Sci.*, **60**, 607–625.
- Lappen, C.-L., and D. A. Randall, 2001a: Toward a unified parameterization of the boundary layer and moist convection. Part I: A new type of mass flux model. *J. Atmos. Sci.*, **58**, 2021–2035.
- , and —, 2001b: Toward a unified parameterization of the boundary layer and moist convection. Part II: Lateral mass exchanges and subplume-scale fluxes. *J. Atmos. Sci.*, **58**, 2036–2051.
- , and —, 2001c: Toward a unified parameterization of the boundary layer and moist convection. Part III: Simulations of clear and cloudy convection. *J. Atmos. Sci.*, **58**, 2052–2072.
- , and —, 2005: Using idealized coherent structures to parameterize momentum fluxes in a PBL mass–flux model. *J. Atmos. Sci.*, **62**, 2829–2846.
- Launder, B. E., 1975: On the effects of a gravitational field on the turbulent transport of heat and momentum. *J. Fluid Mech.*, **67**, 569–581.
- , G. J. Reece, and W. Rodi, 1975: Progress in the development of a Reynolds stress turbulent closure. *J. Fluid Mech.*, **52**, 609–638.
- Mason, P. J., 1989: Large-eddy simulation of the convective atmospheric boundary layer. *J. Atmos. Sci.*, **46**, 1492–1516.
- McBean, G. A., and J. A. Elliot, 1975: Vertical transports of kinetic energy by turbulence and pressure in boundary layer. *J. Atmos. Sci.*, **32**, 753–766.
- Moeng, C.-H., 1984: A large-eddy-simulation for the study of planetary boundary-layer turbulence. *J. Atmos. Sci.*, **41**, 2052–2062.
- , and P. P. Sullivan, 1994: A comparison of shear- and buoyancy-driven planetary boundary layer flows. *J. Atmos. Sci.*, **51**, 999–1022.
- Rotta, J. C., 1951: Statistische theorie nichthomogener turbulenz I. *Z. Phys.*, **129**, 547–572.
- Schumann, U., and C.-H. Moeng, 1991: Plume fluxes in clear and cloudy convective boundary layers. *J. Atmos. Sci.*, **48**, 1746–1757.
- Sykes, R. I., and D. S. Henn, 1988: On the numerical computation of two-dimensional convective flow. *J. Atmos. Sci.*, **45**, 1961–1964.
- Willis, G. E., and J. W. Deardorff, 1974: Laboratory model of the unstable planetary boundary layer. *J. Atmos. Sci.*, **31**, 1297–1307.
- Wyngaard, J. C., and O. R. Coté, 1971: The budget of turbulent kinetic energy and temperature variance in the atmospheric surface layer. *J. Atmos. Sci.*, **28**, 190–201.
- , and —, 1974: The evolution of a convective planetary boundary layer—A higher order closure model study. *Bound.-Layer Meteor.*, **7**, 289–308.
- Yamada, T., and G. Mellor, 1975: A simulation of the Wangara atmospheric boundary layer data. *J. Atmos. Sci.*, **32**, 2309–2329.
- Young, G. S., 1988: Turbulence structure of the convective boundary layer. Part II: Phoenix 78 aircraft observations of thermals and their environment. *J. Atmos. Sci.*, **45**, 727–735.
- Zeman, O., and J. J. Lumley, 1979: *Turbulent Shear Flows*. Vol. 1, Springer, 295 pp.